Encapsulation of Polyoxometalates in Metal-Organic Frameworks and their Applications

A dissertation submitted to the Department of Chemistry, Quaid-i-Azam University, Islamabad, in partial fulfillment of requirements for the degree of

Master of Philosophy

in

Analytical/Inorganic Chemistry

by

Zonish Zeb
Reg. No.02061611008
Department of Chemistry
Quaid-i-Azam University
Islamabad
2016-18

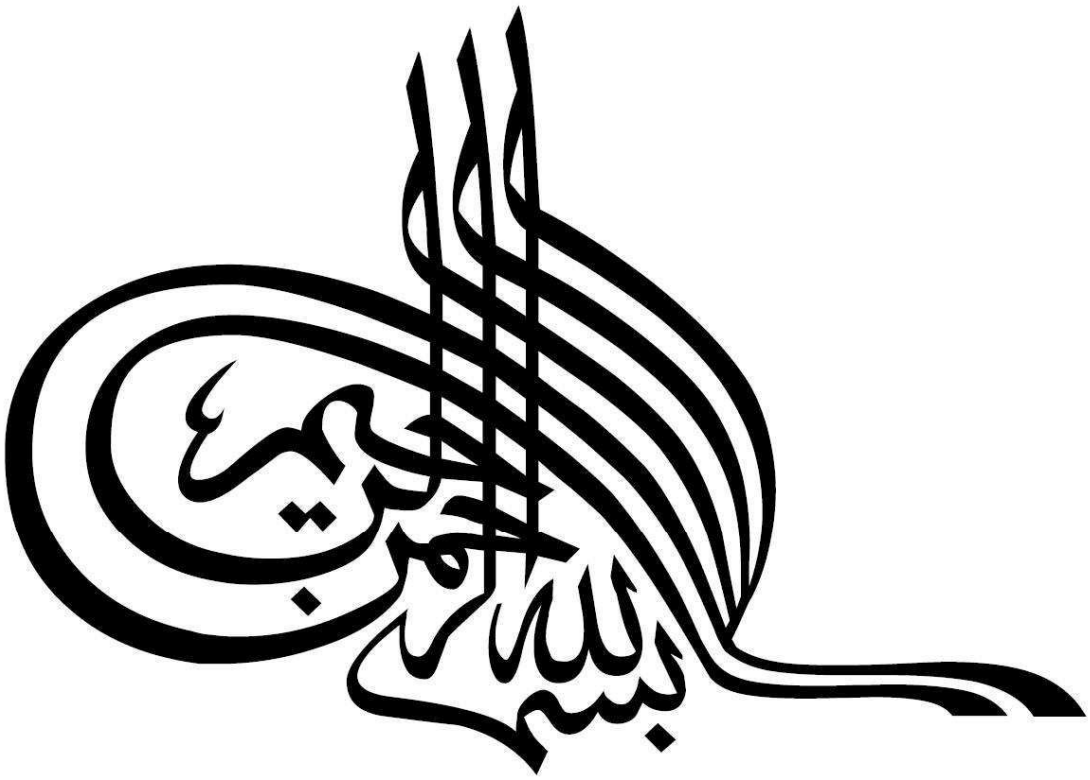

In the name of Allah,
the Most Beneficent,
the Most Merciful

I dedicate this thesis to

the Holy Prophet Hazrat Muhammad (PBUH)

Who is WELL WISHER of us and His teachings are the light of life in this world and world hereafter.

To my father, Aurangzeb

and

To my mother, Jamila Naz

Acknowledgements

In the name of Almighty Allah, the most Gracious and The most Merciful, all the praises to Almighty Allah, for the strength in completing this task. May the blessings of Allah be upon the Holy Prophet Hazrat Muhammad (PBUH) and his family and his noble companions.

My special appreciation is for my supervisor, Dr. Muhammad Arif Nadeem for his kind supervision and constant support, constructive comments and suggestions throughout the research work and thesis. Thank you so much sir!

I am also thankful to Head of Department of Chemistry Dr. Muhammad Siddiq and Head of Analytical/Inorganic section Dr. Amin Badshah for providing facilities to complete my M.Phil studies.I also present my thanks to my senior Waqas Ali Shah (PhD Scholar) for his ever - available guidance, help in research work, encouragement and facilitating during the whole research work.

I am also thankful to my friends Kokab Nazim, Fareena Dar, Mehwish Bashir, Amina Maryam, Attiya, Madiha Saqlain, Neelum , Samina and Benish Ayub for their unconditional support.

Finally, my family, my father, mother, sister (Farhana) and brothers (Adil, Fazil and Zohaib) whose constant support and encouragement made me to undertake this study.

(ZONISH ZEB)

Contents

List of Figures

List of Tables

Abbreviations

POMs	Polyoxometalates
MOFs	Metal Organic Frameworks
POMOFs	POMs/MOFs composites
Hmim	2-methylimidazole
DMF	Dimethylformamide
PXRD	Powder X-ray diffraction technique
FTIR	Fourier Transform Infrared Spectroscopy
TGA	Thermogravimetric analysis
TG	Thermogravimetry
PW_{12}	12-tungstophosphoric acid
PW_{11}	11-tungstophosphoric acid
SiW_{11}	11-silicotungstic acid
ICP-MS	Inductively Coupled Plasma Mass Spectrometry
4-NP	4-nitrophenol
4-AP	4-aminophenol
PNP	Paranitrophenol
CR	Congo red

Abstract:

Four POMOF composites are synthesized by encapsulating polyoxometalates in metal organic frameworks which include $H_3PW_{12}O_{40}.24H_2O$@ZIF-8 (A-1), $K_7[PW_{11}O_{39}].12H_2O$@ZIF-8 (A-2), $K_3SiW_{11}O_{39}$@Neodymium MOF (A-3) and $H_3PW_{12}O_{40}.24H_2O$@MOF-5 (A-4). The POMOF composites are successfully characterized and confirmed by Powder XRD, FTIR, TGA and N_2 adsorption studies. The results show the successful encapsulation of POMs in MOFs. The synthesized POMOF composites are used for catalytic applications which include 4-nitrophenol reduction and degradation of Congo red dye. A-2 is found to be active for 4-NP reduction to 4-AP at pH 5 while A-3 is slightly active for 4-NP reductionA-2 and A-3 are active for catalytic dye degradation of Congo red dye.

1 Introduction

This chapter covers the brief introduction of polyoxometalates (POMs), metal organic frameworks (MOFs) and the problems associated with homogeneous catalysis of POMs and their solutions to make POMs heterogeneous catalysts.

1.1 Overview of Polyoxometalates (POMs):

Generally, POMs are formed of building blocks of metal-oxide MO_x in which 'M' is V, W, Mo etc. called as addenda. Almost all clusters of POMs are anionic and can form the complexes with other cations (P^{5+}, As^{5+}, Si^{4+}, Ge^{4+}, B^{3+}, etc.) which are called heteroatoms. The heteroatom can be of two types; primary or secondary. The primary heteroatom is important part of POM structure but not present in centre always. Partial decomposition of the parent compounds results into the lacunary structures which have vacancies that can be filled by external cations. These cations are called secondary heteroatoms. Larger aggregate of structures of POMs results by further linking of POMs by these heteroatoms or cations.[1]

1.2 History of Polyoxometalates:

In 1826, Berzelius discovered the first heteropoly salt called as ammonium 12-molybdophosphate.This invention gave rise to chemistry of POMs.[2] Up till now so many POMs have been discovered and their structure remained a mystery for a century after their discovery. Werner, Miolati, Rosenheim and Pauling proposed their structure on basis of sharing of metal-oxygen polyhedral.[3] After 20 years of discovery of ammonium 12-molybdophosphate, Svanberg and struve showed that this complex formed insoluble salts which can be used for analysis of phosphates through gravimetric analysis. In 1862, Marignac discovered tungstosilicic acids along with their salts which resulted in flourishing of POMs chemistry.[4] In 1929, L. C. Pauling proposed structure of 12-phosphotungstoacid formed by XO_4 tetrahedral surrounded by twelve MO_6 octahedra . To reduce electrostatic repulsions, polyhedral linkages were sharing vertices instead of edges. Hence, the formed structure involved 58 oxygen atoms with formula $[(PO_4)W_{12}O_{18}(OH)_{36}]^{3-}$. [3] In 1933, Keggin introduced 12-phosphotungstic acid structure

on basis of interpretation of PXRD pattern. The anion was based on WO_6 octrahedral units linked by shared edges and comers.[5] In 1934, Signer and Gross showed that $H_5BW_{12}O_{40}$, $H_4SiW_{12}O_{40}$ and $H_6[H_2W_{12}O_{40}]$ were structurally isomorphous with Keggin's structure. [6]

1.3 Classification of POMs:

There are many structures which comes under the definition of POMs hence it is difficult to classify the POMs but they can be classified on basis of physical properties, structure and main building block types.

1.3.1 Isopolyoxometalates:

Isopolyoxometalates are generally represented as $[M_mO_y]^{p-}$. They are generally synthesized by reaction of transition metal ions $[MO_4]^{n-}$ and protons.[7] Usually, heptamolybdate is formed as;

$$7[MoO_4]^{2-} + 8H^+ \rightarrow [Mo_7O_{24}]^{6-} + 4H_2O$$

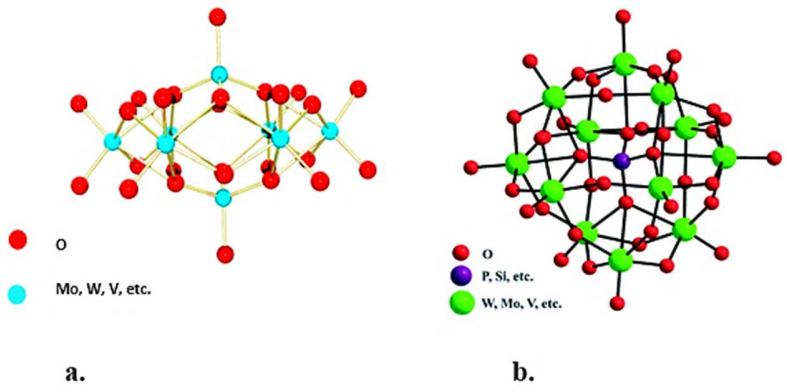

Figure 1.1: a. Isopolyoxometalate b. Heteropolyoxometalate

1.3.2 Hetero-polyoxometalates:

Heteropolyoxometalates are representated as $[X_xM_mO_y]^{q-}$. These consist of one or more than one X (hetero atoms) along with M (transition metals) such as W, V, Mo etc.

Heteroatoms are elements which belong to s-, p-, d- and f block.[7] General equation for the preparation of phosphododecatungstate:

$$12[WO_4]^{2-} + [HPO_4]^{2-} + 23H^+ \longrightarrow [PW_{12}O_{40}]^{3-} + 12H_2O$$

Structure of isopolyoxometalate and heteropolyoxometalate is shown in figure 1.1.

1.3.3 Lacunary Polyoxometalates:

POMs when placed in basic solutions decompose to give monomeric products but if pH is controlled various other forms of POMs can be obtained by removal of one or more MO_6 octahedra. These are known as lacunary structures.[8] Keggin anions consist of five distinct types of isomers called as "Baker-Figgis" shown in figure 1.2.[9]

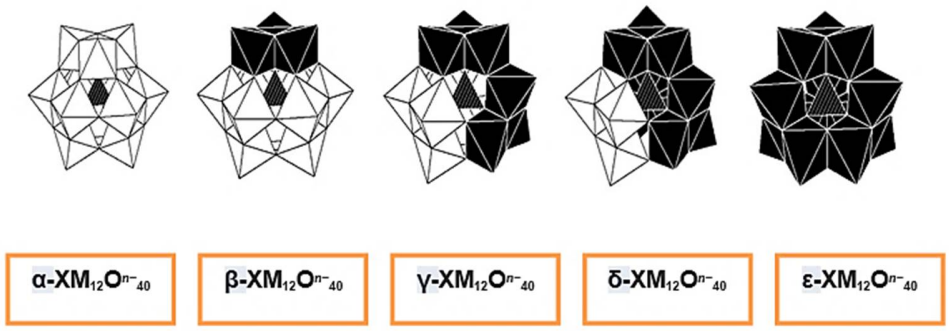

Figure 1.2: Functional isomers of Keggin anion

1.4 Types of POMs on basis of Structure:

Several types of polyoxometalate structures are given below:

1.4.1 Keggin Structure:

The Keggin anions are represented as $[X^{n+}M_{12}O_{40}]^{(8-n)-}$.They possess a central hetero-atom i.e. P, Si, or Ge etc.12 oxygen octahedra bearing Mo, W (addenda atom) surround central hetero-atom. The kinds of oxygen atoms present in Keggin structure are shown in figure 1.3.[10]

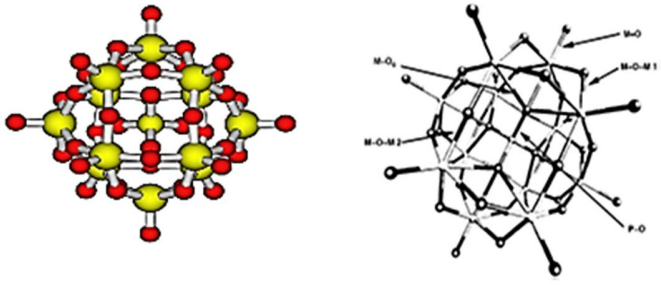

a. b.

Figure1.3: a. Keggin structure b. Keggin structure with P-O showing bond of oxygen central metal atom, M-O-M represents metal oxygen bonds in bridging mode, M=O shows metal oxygen terminal bonds.

1.4.2 Wells–Dawson Structure:

It is generally shown as $[X_2M_{18}O_{62}]^{n-}$, Mo or W may be present as M.A tetrahedral unit is represented by X. Firstly it was given by Wells in 1945. Later, it was studied in 1953.Under acidic media, Kegging anions i.e. $[XM_{12}O_{40}]^{3-}$ tend to lose three octahedrons. The complex anion forms by the two species which are consisting of identical halves linked to each other through oxygen atoms. Nine MO_6 octahedron are surrounding the heteroatoms.[11-12] Well Dowson structure is shown in figure 1.4.

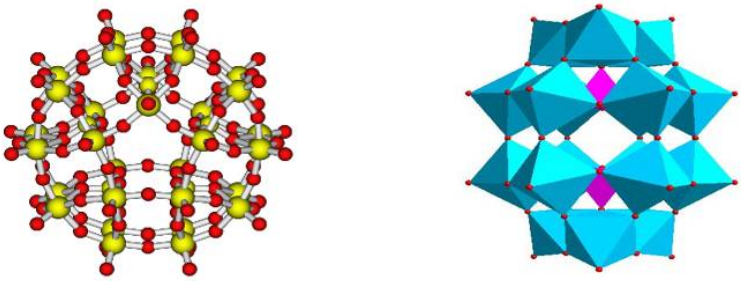

Figure 1.4: Wells-Dowson structures

1.4.3 Anderson Structure:

This structure consists of six MO_6 Octahedra which are co-planar surrounding the central octahedron. Central heteroatom contains six oxo ligands and seven octahedra sharing edges. Central heteroatom can be Te, I, Co, Al.[13] Figure 5 shows Anderson structures.

Figure 1.5: Anderson Structures

1.4.4 Anderson-Evan Structure:

The structure is represented by general formula $[H_y(XO_6)M_6O_{18}]^{n-}$, where *y* can be from 0 to 6, *n* can be from 2 to 8, addenda atoms (Mo^{VI} or W^{VI}) are represented as M, X is central heteroatom. Structure of $[TeMo_6O_{24}]^{6-}$ is called Anderson-Evan structure which was proposed by Anderson and confirmed by Evan in 1948 using single crystal X-ray diffraction technique.[14-15] Aderson-Evan structure is shown in figure 1.6.

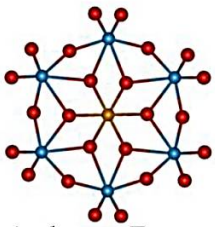

Figure 1.6: Aderson-Evans structure

1.4.5 Lindqvist Structure:

This structure consists of isopolyanion $[M_6O_{19}]^{n-}$ consisting of six MO_6 octahedra

arranging themselves in octahedron shown in figure 1.7. Octahedrally coordinated metal centres are present and terminal metal oxygen bonds are short as compared to bridging metal oxygen bonds.[16]

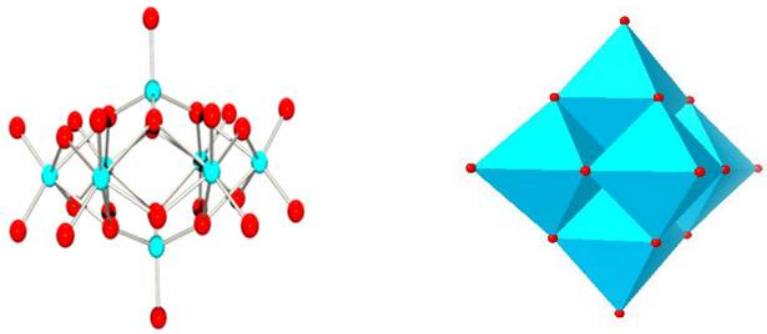

Figure 1.7: Lindqvist structures

1.5 Properties of POMs:

1.5.1 Bronsted Acidity:

The POMs are strong Brønsted acids. They are used as catalysts for various acid catalysed reactions at industrial level, for example, alkylation and hydration of alkenes etc.[17] POMs exhibit different redox and acid base properties by varying their composition for example, variation in hetero-atoms or addenda atoms[18]. In aqueous solutions POMs are strong acids, also higher acidic strength than Oxo acids. Their acidity can be compared to zeolites. The mineral acids such as HCl, HNO_3, HCl, H_2SO_4 are weaker acids as compared to POMs.[19] Table 1 shows the acidic strength.

1.5.2 Lewis acidity:

Lewis acidity depends upon the electropositive character of metal cations. Stronger acidity is observed when electropositivity values are high.[20,21]

1.5.3 Basic Properties of Polyoxometalates:

The basic properties of polyoxometalates depend upon the oxygen atoms of POMs, size and charges of anions, structure and other elements which are the part of structure.

Oxygen atoms present at POMs surface are more active catalysts therefore, go for base catalyzed reactions.[22]

Table 1: acidic strength of some POMs

Acid	pK_1	pK_2
$H_3PW_{12}O_{40}$	1.6	3.0
$H_4PW_{11}VO_{40}$	1.8	3.2
$H_4SiW_{12}VO_{40}$	2.0	3.6
$H_3PMo_{12}O_{40}$	2.1	3.6
$H_3PMo_{12}O_{40}$	6.6	3.9
HCl	4.3	
HNO_3	9.4	

1.5.4 Redox Properties:

POMs show exceptional chemical properties of multi-electron transfers reversibly in multistep. Redox properties depend upon:

- Central atom
- Addenda atom
- Counter ions

The decrease in oxidation potential for HPAs in case of addenda atoms is given as V>Mo>W, while for central atom, P>Ge>Si.[23,24] POMs are reduced easily, e.g. $[PMo_{12}O_4]^{3-}$ can accept 24 electrons to form $[PMo_{12}O_{40}]^{27-}$ as shown in figure 1.8. They have ability to undergo multiple electron redox processes therefore, they are known as electron sponges.[25]

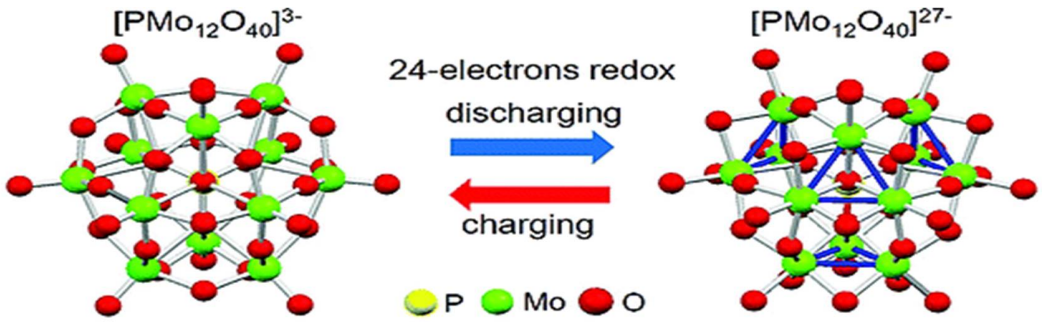

Figure 1.8: Mo^{6+} reduction to Mo^{4+}

1.6 Applications of POMs:

Polyoxometalates have been widely used in many fields due to their higher activities and unique properties. These are used in many fields which include medicines[26], energy storage devices[27] and as dye degradation catalysts.[27] About 80 to 85% applications of POMs are as homogeneous and heterogeneous catalysts.[28]

1.6.1 Catalysis:

Catalysis is the significant field of POMs applications, many POMs are used as catalysts. For example, their uses in water splitting purposes. A tetraruthenium POM was used in combination with a Ru $(bipy)_3^{3+}$ or Ce(IV) for quick water oxidation catalysis at ambient temperature in water. The catalyst having formula $[\{Ru_4O_4(OH)_2(H_2O)\}(g\text{-}SiW_{10}O_{36})_2]^{10-}$ possessed high turnover frequency and low overpotential.[1]

1.6.2 Base Catalysis:

Recently POMs have been found effective for many base catalysed reactions such as carbonyl compounds cyanosilylation, carbon-carbon bond forming reactions and CO_2 fixation.[22]

1.6.3 Acidic Catalysis:

They show Bronsted and Lewis acidity hence are employed in acid catalysed processes which involve transesterification, hydrolysis and Friedel-Crafts alkylation and acylation.[29]

1.7 Metal Organic Frameworks:

MOFs are networks extended in three-dimensional space which bear crystallinity with large pore openings up to 98Å. They have low densities up to 0.13 g cm^{-3}. They bear high surface areas which ranges to 10, 400 m^2 g^{-1} which make them useful. These are the solid materials having the everlasting pores. They consist of either metal clusters or metal ions called nodes and bridging ligands i.e. organic linkers and form the three dimensional coordination structures.[30-31] Figure 1.9 shows general representation of formation of MOFs.

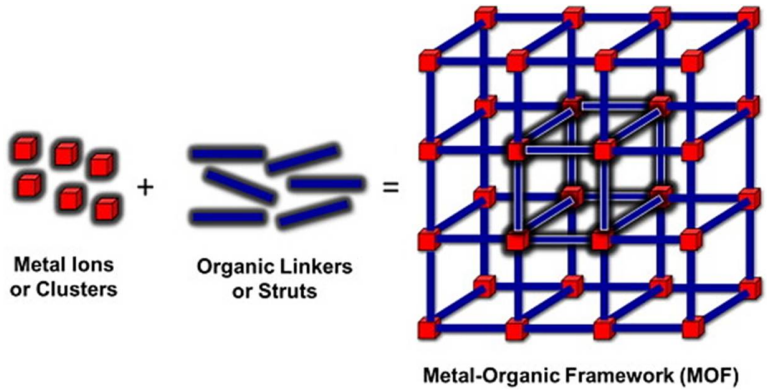

Figure 1.9: General representation of formation of MOFs

1.7.1 Design of MOFs:

Secondary building units (SBUs) are the moieties in which metal coordination surroundings and coordinating behaviour of ligand help in conversion of these moieties to wide porous 3-D structures along with poly-topic linkers. The method of synthesis usually consists of mixing solution of the hydrophobic organic linker with solution of hydrophilic metal mainly by two methods;

- Solvothermal or
- Hydrothermal methods of synthesis

Other methods of synthesis are given in figure 1.10. In the synthesis of MOFs, huge varieties of metal species, i.e., transition metals, rare earth and alkaline earth elements have been effectively utilized with their stable oxidation states. Preference is given to the rigid organic linker systems as compared to flexible as they yield porous, stable and crystalline MOFs. Commonly used linkers are poly-azaheterocycles and Poly-carboxylic molecules[31].Interactions of the metal ion and the organic linker vary to large extent. These interactions are found to ionic, covalent, and coordinate in nature.[32] π-π interactions and Hydrogen bonding are also present.[33] Overall stability of the formed metal organic framework depends upon these interactions.

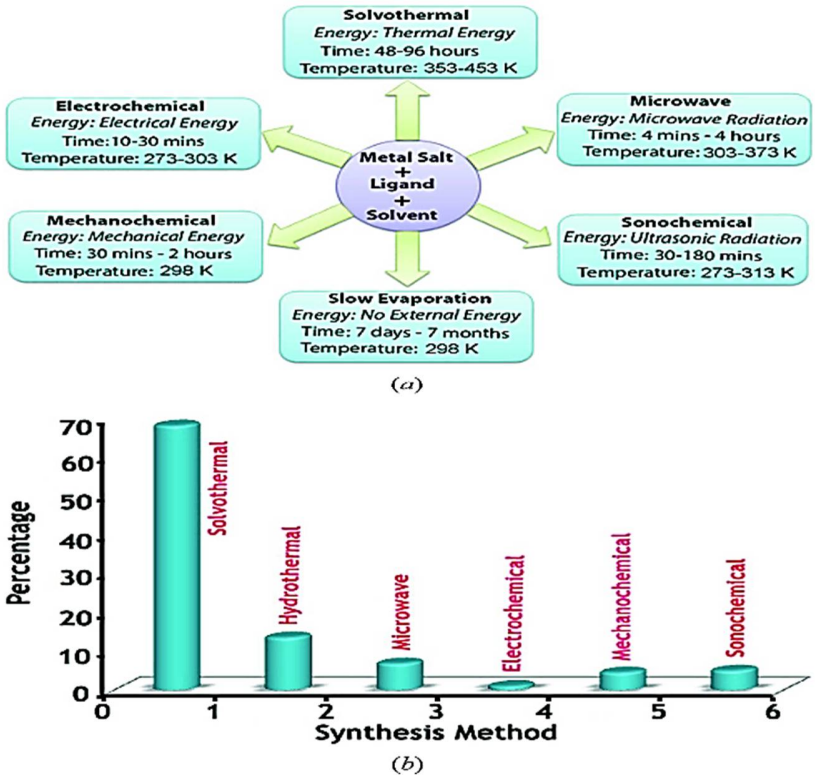

Figure 1.10: Methods of synthesis of MOFs

1.8 Properties of MOFs:

1.8.1 Porosity:

MOFs are porous having different sizes of pores, mostly microporous pore size ranges from 5 to 20 Å. Mesoporous MOF materials are also found.[34] Table 2 shows different pore sizes of MOFs.

Table 2: Different pore sizes

Pores	Pore size in Å
Macro-porous	>500
Mesoporous	20-500
Ultra-microporous	<5
Microporous	5-20

Pores are large and can accommodate smaller moieties but cannot permit larger moieties as proteins.[35]

1.8.2 Chemical and Thermal Stability:

MOFs consist of strong bonds including C-C, C-O, C-H and M-O which make MOFs thermally stable. Their thermal stability ranges from 250 °C to 500 °C.[35] TGA and thermodiffraction analysis give information about thermal stability of the MOFs. These analyses are performed in a stream of air or inert gases such as, He or N_2 with temperature increased from 850 to 1000 K. This temperature is sufficient for complete destruction of MOF. Many MOFs are thermally stable above 573 K. Hence, they can be used in inclusions in liquid phase reactions which take place below 473 K.[36]

1.8.3 Persistency in Microporosity:

When the solvent is evacuated from MOFs, the microporosity of the MOFs is persistence.[37]

1.8.4 Pores and Channel size:

The pores of the MOFs exhibit uniformity and their size of channel is controllable hence, employed in heterogeneous catalysis. They possess synthetic flexibility.[38]

1.9 Applications of MOFs:

MOFs have high porosity and variety of potential applications including their utilization in energy systems like fuel cells and supercapacitors. Their use in catalysis made them important material. These are applied for following purposes;

Gas storage[39]

Gas purification[40]

Photoluminescence[41]

Photo catalysis[42]

Drug delivery[43]

Molecular sensing[44]

Molecular based magnetisms[45]

Biomedicine[46]

Figure 1.11 shows various applications of MOFs in different fields of daily life.

1.10 Catalysis by MOFs:

MOFs have broad range of applications in catalysis. They possess several active sites, such as, metal centres, organic linkers and some moieties which are encapsulated or immobilize in MOFs. They are used in various organic reactions such as, polymerization, Beckmann rearrangement, Friedlander reaction[47-48], Biginelli reaction, hydroformylation and Sonogashira reaction. Methane conversion into acetic acid by MIL-47 and MOF-48 was observed by Yaghi *et al.* as shown in figure 1.12. These MOFs have Vanadium metal

in them. They show high thermal stability at elevated temperature i.e. 425°C. No deformation of structure is observed during recycling. They show better activity for the reaction therefore, they are employed as active homogeneous catalysts.[31] MOF compounds have three different components which are;

- The metal of MOF
- The organic bridging linker
- The pores and cavities system of MOF

Hence catalytic activity can be due to these components of the MOF systems. Either of these can be active and can aid in catalytic activity.[38]

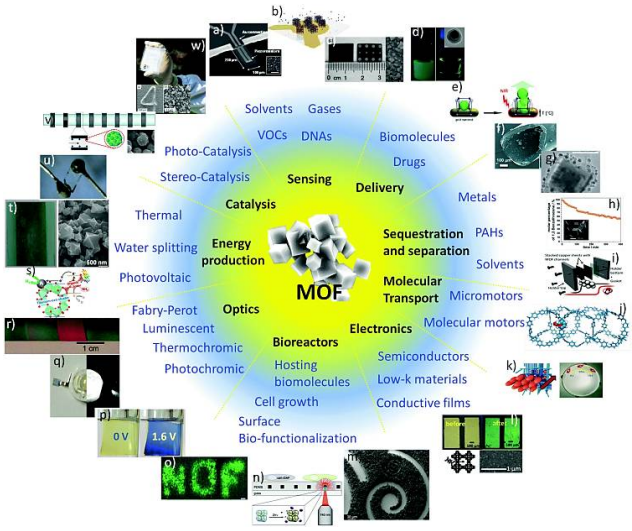

Figure 1.11: Applications of MOF

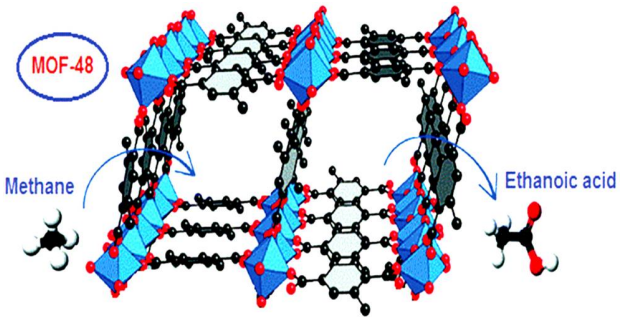

Figure 1.12: Conversion of methane to acetic acid

1.11 MOFs as heterogeneous Catalysts:

The catalysis carried out by MOFs depends upon the active centres present in MOF that aid in catalysis. Hence, metal centres as well as organic linkers of MOFs both play role in catalytic performance of the MOFs. The bridging organic moieties of the MOFs can serve as a platform for encapsulating many homogeneous catalysts, biomolecules and complexes to convert them to heterogeneous catalysts. The pores of the MOF can be used as guest hosts for catalysts which are active in homogeneous catalysis. Controllable pore sizes and environment of pores can be achieved through flexible synthesis of MOFs. MOFs are being used in many fields as active catalysts which are heterogeneous because of various advantages.[31]

- The catalyst can be reused
- Separation of product is facile
- Leaching issues are less

MOFs are used as heterogeneous catalysts. There are various strategies for inclusion of the homogeneously active moieties into the scaffolds of the MOFs. MOFs are among highest porous materials, their chemical environment, pores and cavity size, shapes and dimensions are tunable. Versatility of the MOFs enables them to be the fruitful in catalysis reactions. Activation of organic and inorganic moieties for heterogeneous catalysis by MOFs can follow:[36]

- Direct synthesis of contemplate scaffold
- Post synthetic modifications
- Encapsulation inside the cavities and pores of the MOFs

Several MOF based Hybrids Materials are being synthesized by using various strategies in figure 1.13.

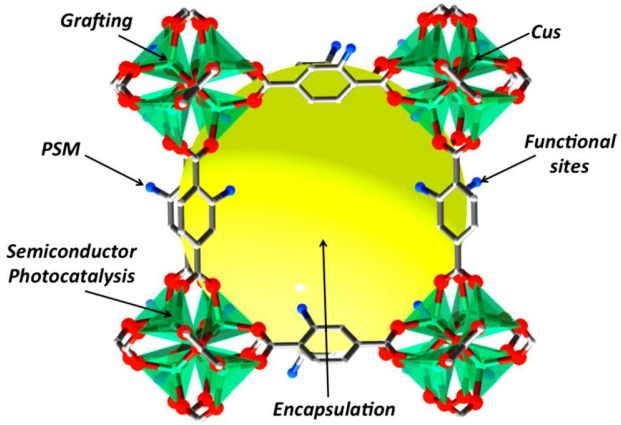

Figure 1.13: Various methods for inclusions in MOF species

1.12 POMs as Heterogeneous Catalysts:

POMs belong to group of metal oxides and have excellent redox and acid-base properties in which modifications can be brought according to desire. Hence these can be employed in many fields for different purposes especially in field of catalysis. POMs can be utilized as homogeneous. These can go for heterogeneous catalysis too. In case of homogeneous POMs catalysts they have high catalytic activity but their recovery is low. When POMs are tuned to heterogeneous catalysts, their separation and recovery is high. They are the anionic oxygen metal clusters, sizes ranging to nanometre and even to micrometre. Many attempts have been made on conversion of POMs to heterogeneous catalyst. Many POM based heterogeneous materials have been synthesized characterized and being applied to different fields such as medicine and life sciences, electrochemistry, magnetic chemistry, photochemistry, catalysis, analytical chemistry and material science. Polyoxometalates especially heteropolyoxometalates (HPAs) are being used as heterogeneous catalysts during past two decades in field of catalysis. POMs show very good Bronsted acidity hence can be used in various acidic reactions e.g. transesterification, hydrolysis, esterification, Beckmann rearrangement and Friedel-Crafts alkylation and acylation. Some POMs also have basic properties and can go for basic catalysis and are being employed in various base-catalytic reactions which are oxidation of alcohols, olefins, aromatics, alkanes etc. The acid/base strength, solubility of polyoxometalates in aqueous

and organic solvents and their redox potential can be modified for different purposes by bringing variations their structures and compositions.[38]

1.13 Drawback of Catalysis of POMs as Homogeneous Catalysts:

POMs are successfully used for various applications as efficient homogeneous catalysts. But there are some drawbacks which leads to the formations of POMs based heterogeneous catalysts. These drawbacks are:[49]

- Their solubility in polar solvents
- Low recovery of catalysts because have high solubility in aqueous and organic media.
- High solubility and low recovery issues therefore, recycling is difficult.
- Separation of product/catalyst is also a big issue.
- Requirements of environmental friendly quick changes and the sustainable developments are not fulfilled by heterogeneous POMs catalysts.
- Surface areas are smaller ($<10\ m^2\ g^{1-}$).
- Stability is low under catalytic conditions.

For practical industrial applications the recoverable and recyclable catalyst is required hence, it is necessary to device the POM-based catalyst for heterogeneous catalysis. Drawbacks of POM based heterogeneous are also present such as;[49]

- Leaching of catalytic sites
- Mass transfer resistance
- Low activity

Many strategies have been given for enhancing the stability and to improve activities in catalysis.[50]

1.14 Synthesis Approaches of POM-based heterogeneous Catalysts:

The two main strategies can be used for preparing POM-based heterogeneous catalysts are;[49]

- Immobilize POMs which are active for catalysis
- Solidification of the POMs which are catalytically active

These two approaches are employed for synthesis of POM based heterogeneous catalysts.

1.14.1 Immobilizing POMs on Porous Supporting Materials:

Immobilizing the POMs which are active catalysts, onto the porous material which acts as a support, is an easy and quick method to devise POM based heterogeneous catalyst. In this case the substrate requires diffusion through boundary layer of the surrounding solid to the active sites before the intra-particle chemical adsorption and diffusion takes place. And desorption of the product is also required by the reverse process in case of heterogeneous catalysis. Hence in this case the catalytic activity is influenced by the pore structure which plays a vital role in the catalysis, also influence actual catalytic activity and affect the selectivity. Pore structure includes;[49]

- Volume and distribution
- Pore Size
- Micro-environmental states of surface which includes hydrophobic/hydrophilic properties etc.

Usually the porous support material is selected for high and uniform distribution of active sites. It reduces mass transfer resistance too.[49] Various porous materials are being employed as support for immobilizing POMs. Some of the porous materials are as follow:[51]

- Mesoporous silica
- Zeolites
- Mesoporous polymers
- Transition metal oxides that are mesoporous
- Mesoporous molecular sieves
- Magnetic nanoparticles

- Porous carbons
- Metal Organic Frameworks

The immobilization is influenced by differences in host/guest interactions hence, the active sites can be immobilized by the various methods including;[52]

- Ion exchange
- Adsorption
- Covalent linkage
- Substitution
- Encapsulation

For designing an active and efficient catalyst it is necessary to select an appropriate support. The fast developments in material sciences are giving rise to materials which are porous and their composition can be tuned. Surface state, size of pores and morphology of the materials enable the synthesis of multifunctional POM based heterogeneous catalysts.[53] Figure 1.14 shows different strategies of synthesizing POM based heterogeneous materials. [49]

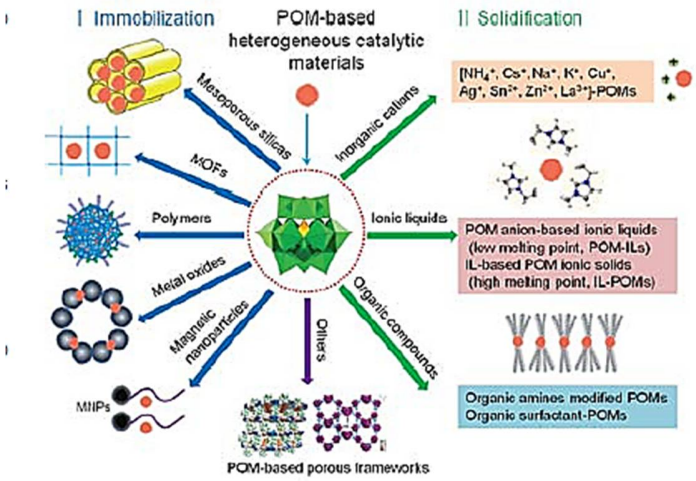

Figure 1.14: Different strategies for synthesizing POM-based heterogeneous materials

1.14.2 Mesoporous silica-based support:

Mesoporous silica-based structures can be used as excellent support for POMs. They have suitable textural parameters which involve;

- Large surface area
- Pore Volume
- Narrow distributions of pores
- Special quantum size effect

SBA-15 is common mesoporous silica which is ordered and its pore size can be varied from 5 to 30 nm by making variations in synthetic conditions of the material. Mesoporous silica has series of families that have been successfully prepared and their pore size and pore volume can be tuned along with adjustment of symmetries. They have wide use as supports for immobilizing POMs for heterogeneous catalysis.[54] Various methods are used for preparing POM based mesoporous silica materials which include;[54]

- Covalent Grafting
- Impregnation
- Sol-gel Techniques
- Ion exchange
- Electrostatic interactions

1.14.3 Porous polymer as support:

Porous polymeric materials have been utilized as supporting material for POM-loaded heterogeneous catalysts. They have excellent properties such as easy processability, tunable structure and functionality. They are suitable due to ductile nature, low weight and facile production.[55] Leng and Wang *et al.* designed many POM based polymeric materials which can be employed as heterogeneous catalysts in esterification, alcohols oxidation and benzene hydroxylation. Figure 1.15 shows schematic diagram of preparation of water tolerant catalyst formed by immobilization $H_3PW_{12}O_{40}$ in organomodified SBA-15.[55]

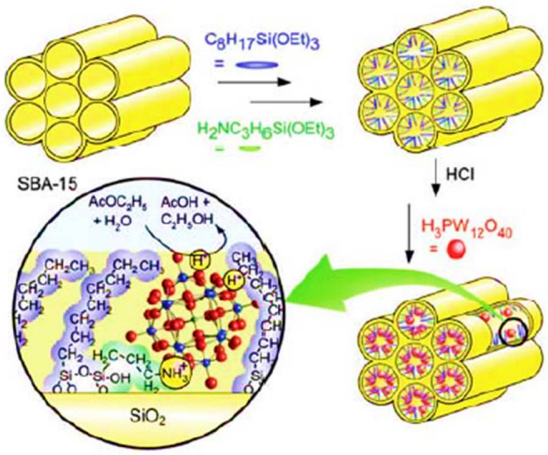

Figure 1.15: Schematic diagram of preparation of water tolerant catalyst formed by immobilization $H_3PW_{12}O_{40}$ in organomodified SBA-15.

1.14.4 Mesoporous metal oxides as support:

Different mesoporous metal oxides, such as ZrO_2, Cr_2O_3, Fe_2O_3, ZnO_2 etc. are being used as support for POM based heterogeneous catalysts due to adjustable composition, structure of pores, ability of assisting in strong host/guest interaction for high catalytic activities and inert structure for resistance against corrosion of accommodated moieties.[55]

1.14.5 MOFs as porous support:

MOFs belong to coordination polymers that are porous. They are open frameworks and have excellent ability to encapsulate polyoxometalates because they bear various properties listed below;[55]

- surface area is high
- Porosity is permanent
- Hydrophilic and hydrophobic channel properties are modified or tuned according to desire

Various efforts have been done to immobilize the POMs on support of MOFs for synthesis of fast POM-based heterogeneous catalysts by electrostatic attachment of POM anions inside MOF matrix through anion exchange.[55]

In 2005, Férey *et al* encapsulated $K_7PW_{11}O_{39}$ within the cages of MIL-101 which is a MOF. This material has good stability, large surface area and pores. It has rigidity in structure. $[PW_{11}CoO_{39}]^{5-}$ and $[PW_{11}TiO_{40}]^{5-}$ cobalt/titanium mono-substituted Keggin heteropolyanions were reported by Kholdeeva and co-workers. New series of different POMs supported on MIL-101 (a MOF containing Cr) are synthesized by Balula and co-workers. These heterogeneous catalysts were used in various oxidation reactions, such as oxidation of styrene, oxidative desulfurization and oxidations of cyclooctane. In MIL-101, $H_3PW_{12}O_{40}$ was encapsulated which was used as catalysis of organic processes, for example, esterification reaction of acetic acid and n-butanol, Baeyer condensation, Knoevenagel condensation of benzaldehyde with ethyl cyanoacetate, etc. NENU-*n* series was prepared by Liu and Su *et al.* in 2009. This was synthesized by hydrothermal process i.e. one step reaction of the starting materials. $PW_{12}O_{40}^{3-}$, Keggin anions were alternatingly arrayed in cages of host (HKUST-1) matrix as non-coordinating guests. In 2011, Hill *et al.* encapsulated $[CuPW_{11}O_{39}]^{5-}$ in pores of HKUST-1 form new crystalline compound, $[Cu_3(C_9H_3O_6)_2]_4[\{(CH_3)_4N\}_4CuPW_{11}O_{39}H]$ which was an efficient catalyst for detoxifying sulfur compounds from H_2S to S_8 using atmospheric air only and it gave higher catalytic performance than its precursors (MOF or POM) alone.[55] Duan *et al.* prepared new enantiomorphs Ni-PYI1 and Ni-PYI2 MOFs catalyst possessing both hydrophobic and hydrophilic parts employed in the aryl olefins asymmetric dihydroxylation by incorporation of POM moieties $[BW_{12}O_{40}]^{5-}$ and t L-or D-pyrrolidin-2-ylimidazole, in a MOF framework.[55]

1.15 Kinds of POM-based MOF Materials:

These kinds of materials are called POM based MOF materials and have properties of both.[55]

- POMs are directly part of MOF frameworks
- Encapsulation of POMs within cavities of the MOF

POM based MOF materials are of two types shown in figure 1.16. These types are:[55]

- Single crystal POM based MOFs

- POM loading into MOF structure i.e. POM is encapsulated by MOF

1.15.1 Single crystal POM-based MOFs:

Single crystal POM based moieties are divided into three types.[55]

- Modified POMs based on d/f block elements i.e. metal ions are linking with organic ligands.
- POMs anions as templates are present inside cages of metal organic frameworks.
- Anionic POMs are present along porous organic-inorganic compounds as pillars.

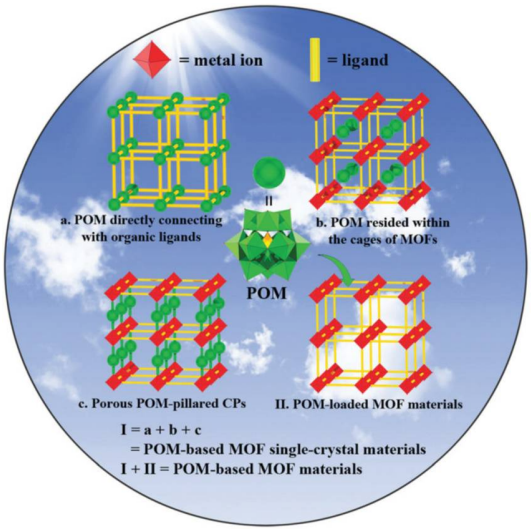

Figure 1.16: Diagram showing POM based MOFs.

1.15.2 MOFs with POMs loading:

MOFs with POMs loading can be prepared by the following three ways;[56]

- POMs are synthesized in the cages of MOF networks.
- By synthesizing MOFs when POMs are also present.
- Impregnating MOFs by a solution of POM

In these three synthetic approaches, second method proves to be excellent for encapsulating POMs into the MOF pores. In case of impregnation, the solution of metal precursors is brought in contact with pores of the MOFs, when impregnated solution

becomes equivalent to volume of pores of MOF, the technique is known as incipient wetness. It requires metal precursor to reduce first to form nanoparticles hence, is not suitable. For reduction, reducing agents can be used.[57]

1.16 Drawbacks of Encapsulation:

Encapsulating the POMs in porous materials have some disadvantages along with many advantages.[57]

- The loading of POMs in MOFs is low.
- Leaching of POMs can also takes place resulting in loss of active sites.
- Agglomeration of particles of POMs may take place.
- Active sites are non-uniform.
- Water deactivates the acid sites.

1.17 Consequences of Encapsulation:

As a result of encapsulation following changes can take place.[58]

- Homogeneous to heterogeneous catalysis
- Improved stability
- Enhanced activity
- Distortion in MOFs structure
- Variations in Pore Structure
- Enhancement in Pores volume
- Loss of crystallinity of MOFs structure

1.18 Advantages of POM-based MOF materials:

Their catalytic use in different applications is due to the several properties.[49]

- These have high thermal stability.
- Recoverable and recyclable after several cycles of applications as heterogeneous catalysts.

- Encapsulation of polyoxometalates in MOFs results in dispersion of POMs. MOFs have high surface area therefore, effective contact between substrate and POM is enhanced by MOF moieties.
- The organic part of the POMOF materials can increase the catalytic performance by influencing lipophilic and hydrophilic properties of catalyst.

1.19 MOFs And POMs Used in Synthesis:

Following MOFs and POMs are used in encapsulation in the current work.

1.19.1 MOFs:

1.19.2 ZIF-8:

ZIF-8 comprises of Zinc metal and ligand is 2-methylimidazole. It formula is $C_8H_{10}N_4Zn$ having pore size 11.6 Å and pore openings 3.4 Å.[59] Figure 1.17 shows structure of ZIF-8.

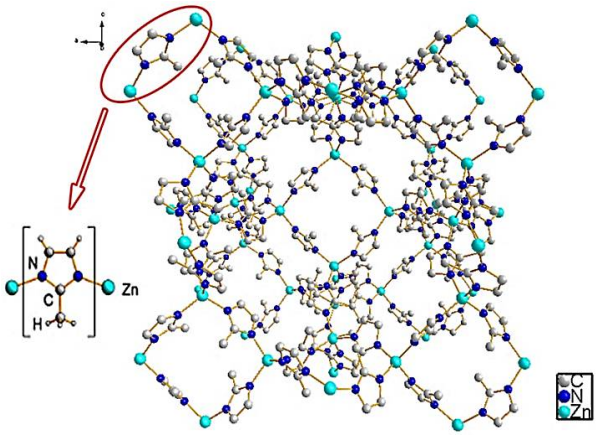

Figure 1.17: ZIF-8 structure

1.19.3 Neodymium based MOF (Nd MOF):

Metal is Neodymium and ligand is pyridine-2,5-dicarboxylic acid.[60]
It has molecular formula: $Nd_8(L)_{12}(H_2O)$. Structure of Neodymium MOF is shown in figure 1.18.

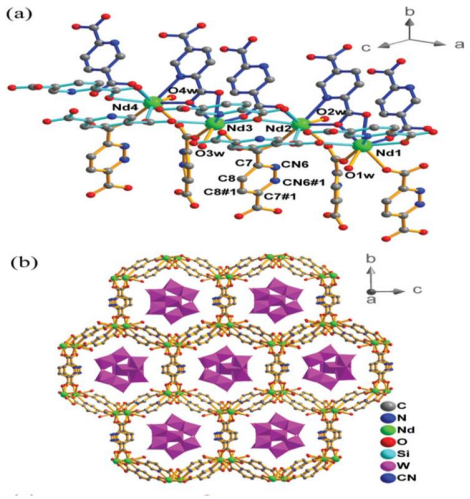

Figure 1.18: Neodymium based MOF structure

1.19.4 MOF-5:

Sometimes it is also called IRMOF-1. Zinc metal is present in MOF-5 along with ligand 1, 4-benzenedicarboxylic acid. Ligand struts are present in between Zn_4O nodes shown in figure 1.19.[61]

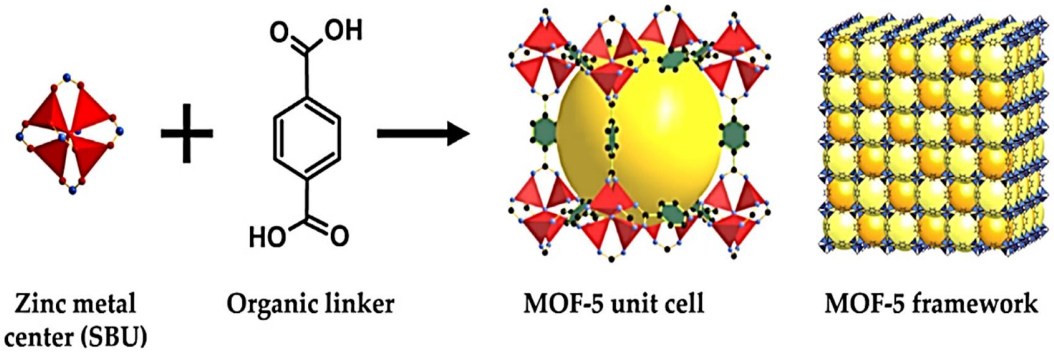

Figure 1.19: MOF-5 structure

1.19.5 POMs Used in Synthesis:

Table 3 comprises of the POMs used in synthesis. Structure of PW_{12} and SiW_{11} are shown in figure 1.20.

Table 3: POMs used in synthesis

Sr. No.	POMs	Type	Size
1.	$k_7PW_{11}O_{39}$ (PW_{11})	Keggin	9.16 Å
2.	$H_3PW_{12}O_{40}$ (PW_{12})	Keggin	10 Å
3.	$K_3SiW_{11}O_{39}$ (SiW_{11})	Keggin	9 Å

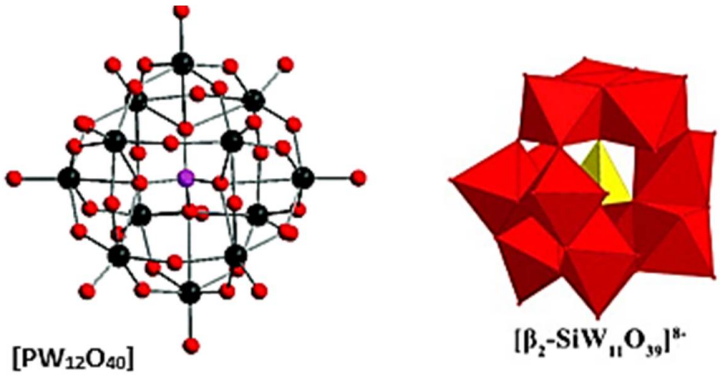

Figure 1.20: Structure of PW_{12} and SiW_{11}

2 Experimental:

The chemicals utilized in synthesis and applications had high purity. Table 4 shows the chemicals used in synthesis.

Table 4: List of Chemicals Used

Serial No.	Name	Chemical Formula
1.	Zinc Nitrate hexahydrate	$Zn(NO_3)_2 \cdot 6H_2O$
2.	Zinc Acetate dehydrate	$Zn(OAc)_2.2H_2O$
3.	Neodymium(III) chloride hexahydrate	$NdCl_3.6H_2O$
4.	11- Silicotungstic acid	$K_3SiW_{11}O_{39}$
5.	12-Tungstophosphoric acid	$H_3PW_{12}O_{40}.24H_2O$
6.	11-Tungstophosphoric acid	$K_7[PW_{11}O_{39}].12H_2O$
7.	Sodium Hydroxide	NaOH
8.	Methanol	CH_3OH
9.	Dimethylformamide (DMF)	C_3H_7NO
10.	Terephthalic Acid	$C_8H_6O_4$
11.	2-methylimidazole	$C_4H_6N_2$
12.	Pyridine-2,5-dicarboxylic acid	$C_7H_5NO_4$
13.	4-Nitrophenol	$C_6H_5NO_3$
14.	Sodium borohydride	$NaBH_4$
15.	Congo red	$C_{32}H_{22}N_6Na_2O_6S_2$
16.	Water	H_2O

2.1 Synthesis of POMOF Composites:

2.1.1 Synthesis of $H_3PW_{12}O_{40}.24H_2O$@ZIF-8 (A-1):

Hmim (1.297 g, 15.7 mmol) and 30 mg of $H_3PW_{12}O_{40}.24H_2O$ were dissolved in 40 mL of

methanol. Zn $(NO_3)_2 \cdot 6H_2O$ (0.5866 g, 1.98 mmol) was dissolved in methanol (40 ml) and quickly poured into solution of Hmim and $H_3PW_{12}O_{40}.24H_2O$ at constant stirring. The ratio of Zn $(NO_3)_2 \cdot 6H_2O$ and Hmim was taken 1:8. Then this mixture was stirred for two hours. The mixture turned turbid slowly and the white precipitates were obtained by centrifugation. Then washing was carried out several times with methanol and air dried.

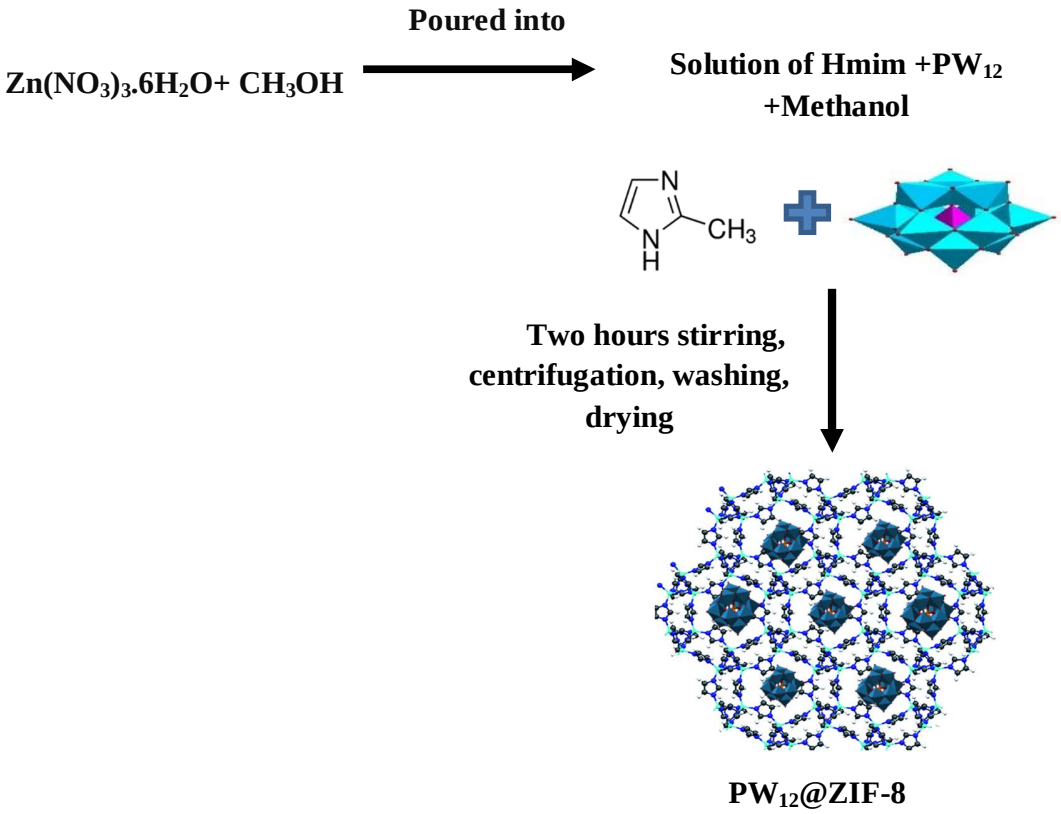

2.1.2 Synthesis of $K_7[PW_{11}O_{39}].12H_2O$ @ZIF-8(A-2):

Firstly, a solution of $K_7[PW_{11}O_{39}].12H_2O$ (30 mg) and Hmim (1.297 g, 15.7 mmol) in 40 mL of methanol was prepared. Then, $Zn(NO_3)_2 \cdot 6H_2O$ (0.5866 g, 1.98 mmol) was added in 40 mL of methanol and this solution was poured into first solution. The ratio of Zn $(NO_3)_2 \cdot 6H_2O$ and Hmim was taken 1:8. The resulting mixture was stir for two hours. Milky suspension was formed and turbidity appeared. The desired product was separated, five times washing was done by methanol and product was dried.

2.1.3 Synthesis of $K_3SiW_{11}O_{39}$@Neodymium MOF(A-3):

A mixture of $NdCl_3 \cdot 6H_2O$ (0.179 g, 0.71 mmol), 2,5-pyridinedicarboxylic acid (0.167 g, 0.99 mmol) and silicotungstic acid ($K_3SiW_{11}O_{39}$) (30 mg) in deionized H_2O (17.5 mL) was prepared and its pH was adjusted 2 with 1.00 M sodium hydroxide. The ratio of $NdCl_3 \cdot 6H_2O$ and 2,5-pyridinedicarboxylic acid was taken 1:1. Then the resulting solution was autoclaved for 3 days. Temperature was maintained at 160 °C The precipitates formed were separated by filtering them, washing was carried out three times by distilled water and DMF.

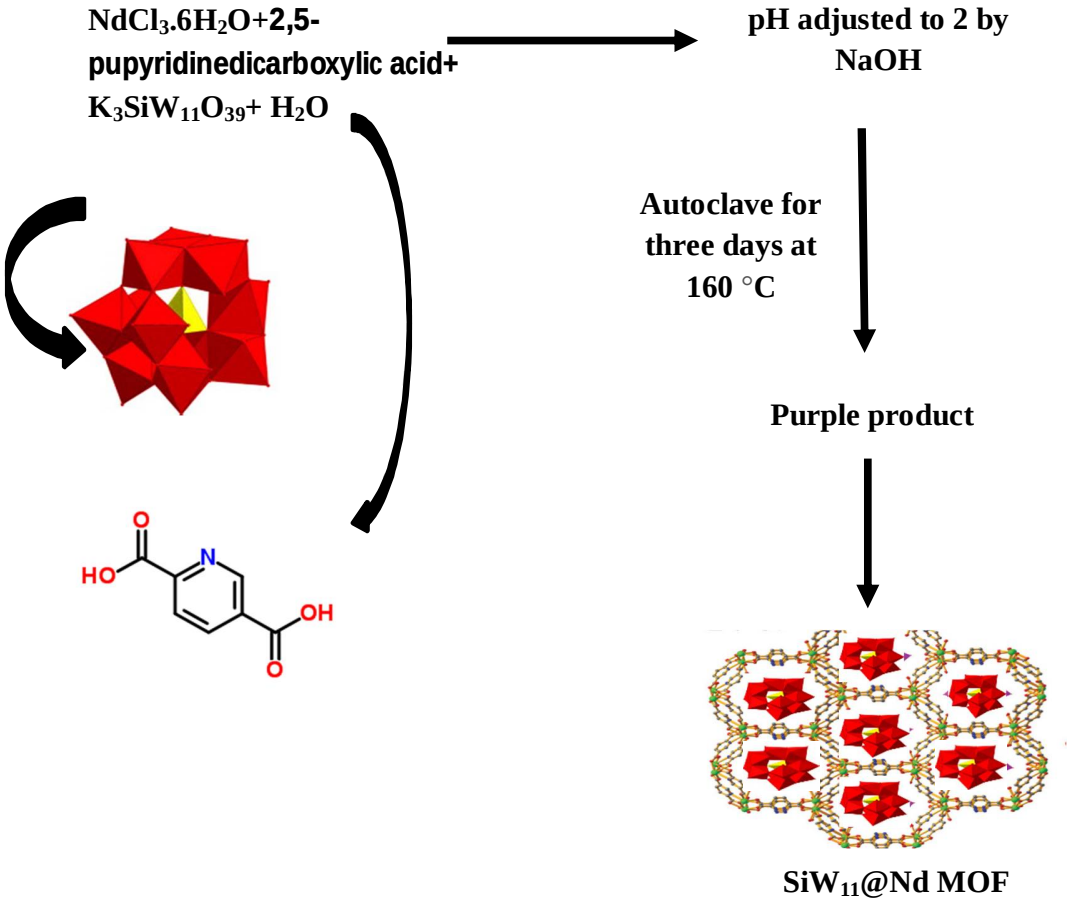

2.1.4 Synthesis of $H_3PW_{12}O_{40}$. $24H_2O$@ MOF-5(A-4):

Terephthalic acid (0.25 g, 1.5 mmol) and $H_3PW_{12}O_{40}.24H_2O$ (30 mg) were mixed in 20 mL of DMF. Another solution was formed by dissolving $Zn(OAc)_2.2H_2O$ (0.84 g, 3.8

mmol) in DMF (25 mL) and added it to the first solution on stirring. The ratio of $Zn(OAc)_2.2H_2O$ and terephthalic acid was taken 2:1. The mixture was left on stirring for 2.5 hours. Precipitates formed were separated by centrifugation, washing was done with DMF and water five times and product was dried.

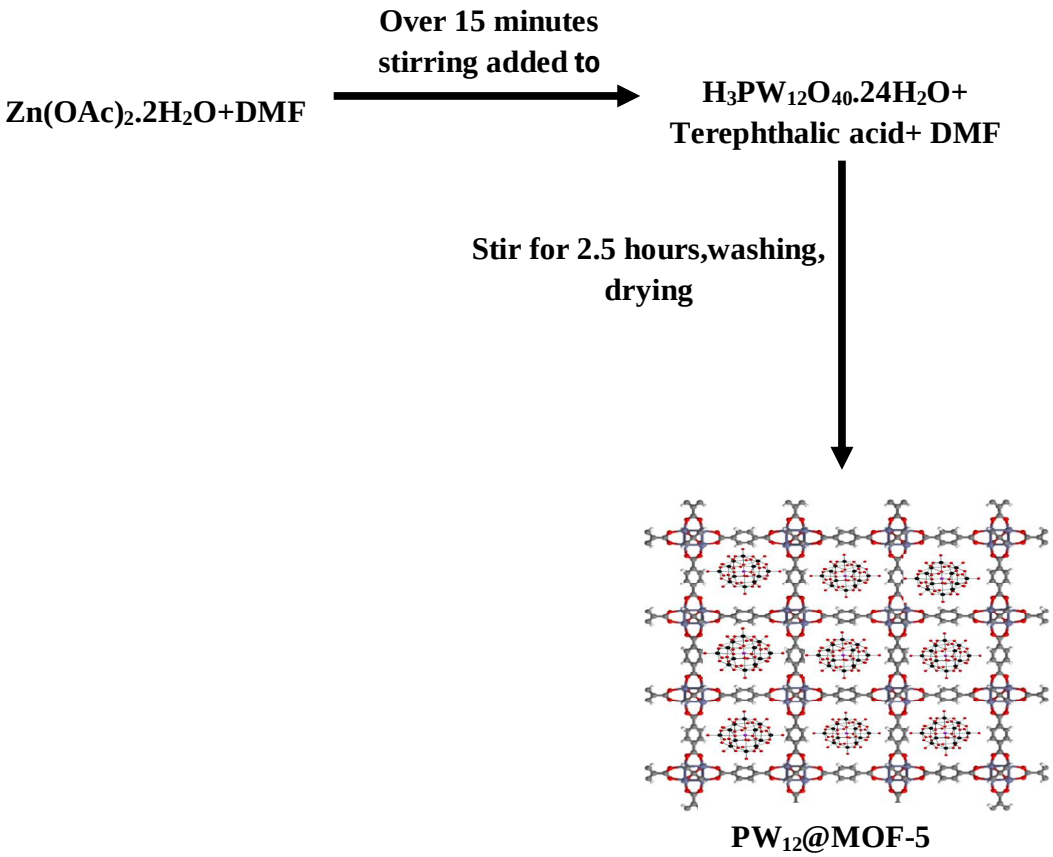

2.2 Characterization:

The synthesized composites of POMs and MOFs were characterized by using different techniques which include FTIR, PXRD, TGA, Elemental Analysis and Nitrogen

Adsorption Studies.

2.2.1 FTIR:

FTIR spectra were obtained by using TENSOR -II Bruker's FTIR Spectrometer ranging

from 4000 to 400cm^{-1}.

2.2.2 Powder XRD:

Diffractograms of samples were recorded by using PAN analytical X´Pert PRO diffractometer. Radiations having frequency 0.015 s^{-1} were used for analysing the samples. 2 theta values were kept from 10 to 80.

2.2.3 TGA:

5E-MAC IV Automatic Proximate Analyzer was employed for thermogravimetric analysis of the samples. The thermal analysis of the samples was ranging from 0 to 500^0C.

2.2.4 Elemental Analysis:

Elemental analyses of the prepared compounds were performed at the Perkin-Elmer 2400 CHN analyser for determination of carbon, hydrogen and nitrogen. For determination of metals ICP-MS was used. Perkin-Elmer Elan 6000 Inductively Coupled Mass Spectrometer was used for analysis.

2.2.5 Nitrogen Adsorption Studies:

Brunnauer-Emmett-Teller (BET) surface adsorption method was used to obtain N_2 adsorption isotherms. BET analyzer instrument was used.

2.3 Studies of Catalytic Applications:

2.3.1 4-Nitrophenol(4-NP) Reduction by synthesized composites:

Commercially available 4-NP was purchased and used for reduction of 4-nitrophenol.

1×10^{-6} M 4-NP aqueous solution and 1mM aqueous solution of $NaBH_4$ prepared. 5 mg of the synthesized composite was added for evaluating catalytic performance. The experiment was performed using 3 mL quartz optical cells. After mixing fresh solutions of $NaBH_4$ and 4-NP, 5 mg of catalyst was added. pH was also adjusted by using HCl.

UV-Visible spectrum was recorded after different time intervals after the addition of catalyst.

2.3.2 Dye degradation studies:

Congo red dye was used for analyzing dye degradation abilities of the composites.

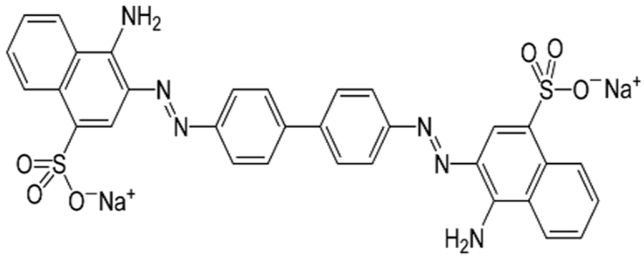

Commercially available Congo red dye $C_{32}H_{22}N6Na_2O_6S_2$ was used for dye degradation studies. $1.7*10^{-4}$ M of dye solution was prepared. Water was used as solvent. Absorption measurements were made by using UV-Visible Spectrophotometer.

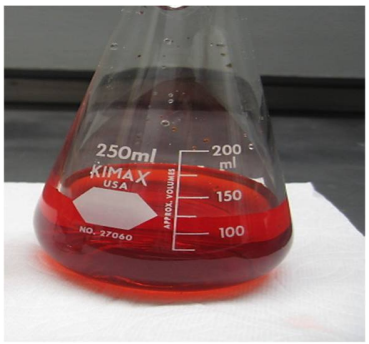

3 Results and Discussion:

Results and discussion includes results of PXRD, FTIR, elemental analysis, TGA and Nitrogen adsorption studies which were used to characterize the synthesized POMOF composites along with the results of catalytic applications of the synthesized composites in 4-nitrophenol reduction and Congo red dye degradation.

3.1 Powder XRD:

Major peaks observed in PXRD spectra of synthesized compounds are matching exactly with the reported MOFs peaks. As POMs are immobilized by MOFs in their cavities due to restricted space hence, POMs do not show diffraction patterns and the PXRD of the synthesized composites of polyoxometalates is based on metal organic frameworks.[60]

3.1.1 PXRD of A-1 and A-2:

PXRD of A-1 and A-2 matches exactly with the PXRD of the reported MOF i.e. ZIF-8 .[62] The PXRD spectra of ZIF-8, A-1 and A-2 are shown in figure 3.1. The appearance of peaks at 32.4°,31.5°, 30.6° , 26.7°, 22.1°, 18.1°, 16.5°, 14.6°, 10.3°and 7.4° confirms the synthesis of A-1 and A-2.[63] Therefore, structure of ZIF-8 is intact after encapsulation.

3.1.2 PXRD of A-3:

Figure 3.2 shows PXRD pattern of A-3 which is exactly matching the PXRD pattern of MOF alone.[60] The peaks observed for Nd MOF exactly match with the peaks of the synthesized compound A-3 which show the integrity of structure of Nd MOF after encapsulation. PXRD confirms the successful synthesis of the MOF after encapsulating POMs inside their cavities. As precursors of MOF i.e. Nd MOF were added along with POMs therefore, PXRD confirms synthesis of Nd MOF without distortion in structure.

3.1.3 Powder XRD of A-4:

The PXRD of composite A-4 exactly matches with the PXRD of reported MOF.[64] The PXRD of A-4 and MOF-5 are shown in figure 3.3. The diffractogram of A-4 has same

peaks as MOF-5 therefore, structural integrity is maintained and MOF-5 structure is intact after encapsulation.

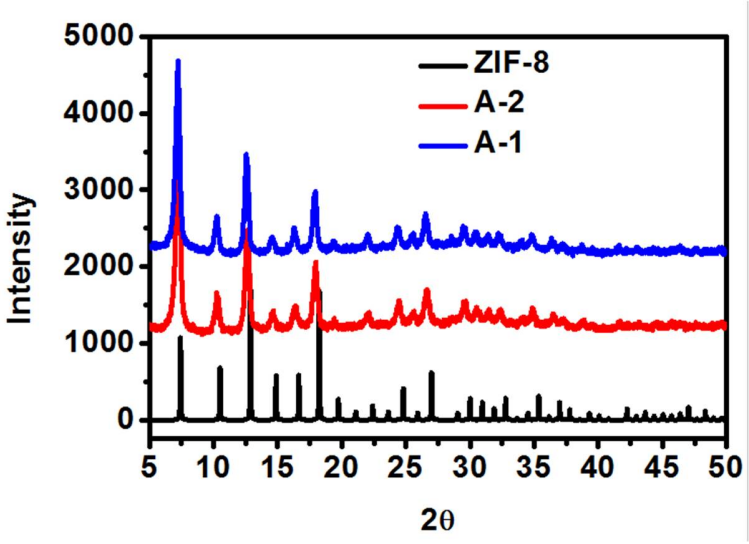

Figure 3.1: PXRD of A-1, A-2 and ZIF-8

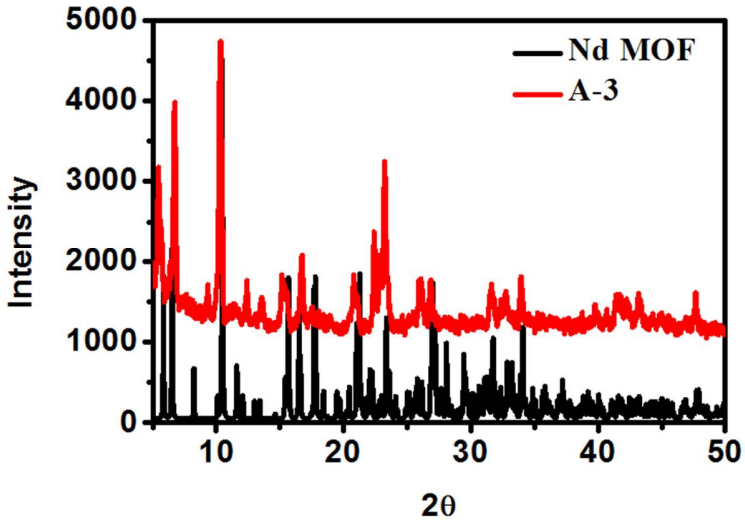

Figure 3.2: PXRD A-3

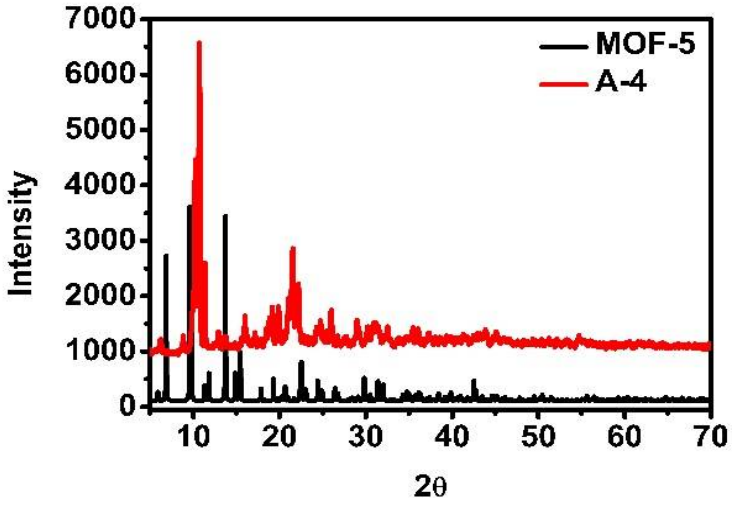

Figure 3.3: PXRD of A-4

3.2 FTIR of the Synthesized POMOF Composites:

FTIR spectrum of all the synthesized POMOF composites and their MOFs and POMs alone were recorded which are given below;

3.2.1 FTIR of A-1 And A-2:

The figure 3.4 shows the FTIR spectra composite materials A-1 and A-2 and ZIF-8. FTIR ZIF-8 spectrum is in agreement with the reported spectrum.[59] IR spectra of A-1 when compared with spectrum of ZIF-8, it showed differences because the bands appeared confirmed the encapsulation of PW_{12} in ZIF-8. The characteristics bands of POM appeared in spectrum of A-1.Edge sharing *v*W-O_c-W is present at 836 cm^{-1}. Appearance of absorption peak at 886 cm^{-1} indicates corner sharing *v*W-O_b-W. Terminal *v*W-O_t appeared at 951 cm^{-1}. *v*P-O peak in PW_{12} is found at 1080 cm^{-1}.[65]

In case of A-2 peaks of POMs are observed along with peaks of MOF. In PW_{11}, P-O bond gives two peaks at 1085 and 1043 cm^{-1}. The peaks observed at 863 cm^{-1} and 808 cm^{-1} are indicating formation of tungsten-oxygen (W-O-W) bond. Appearance of peaks of ZIF-8 along with POM peaks indicates the formation of composite. Aliphatic and aromatic C-H stretch of imidazole appears at 3135 cm^{1-} and 2929 cm^{1-} respectively.[65]

Peak at 1579 cm^{-1} corresponds to stretching mode of C = N.[66] C-N stretch appears in region of 1100–1400 cm^{-1}. [65] Bands in region of 1350–1500 cm^{-1} are stretch of the ring. The bands for the ring's in-plane bending are observed in region of 900–1350 cm^{-1}. Out-of-plane bending is present below 800 cm^{-1} .[66]

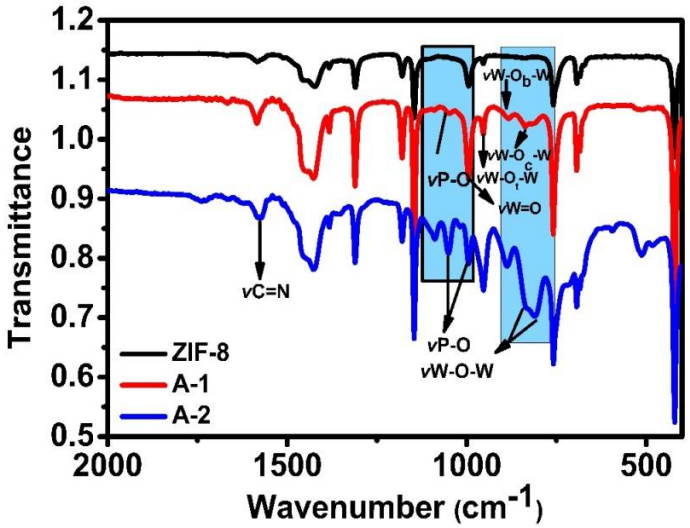

Figure 3.4: FTIR of A-1 and A-2

3.2.2 FTIR of A-3:

In case of A-3 shown in figure 3.5, the characteristic band for silicon oxygen bond stretch (ν Si-O) appear at 920 cm^{-1}.Peaks at 1003 and 950 cm^{-1} show metal-oxygen stretching bands including Si–O and W=O stretching modes, respectively.[60] The absorption bands in between 900 and 600 cm^{-1} are indicating presence of stretching modes of W–O–W bonding. Characteristic absorption bands appearing at 1611, 1581 cm^{-1} and 1396, 1366 $cm^{-1}$are assigned to asymmetric and symmetric stretch of dicarboxylates, respectively. Besides, characteristic peaks of pyridine also appear, which are ν C=N at 1484 cm^{-1},δ CH at 1036 cm^{-1} and γ CH at 804 cm^{-1} .[60]

3.2.3 FTIR of A-4:

Various characteristic peaks of PW_{12} appeared along with MOF-5 peaks in spectrum of

A-3 shown in figure 3.6. *v* W=O peak in PW_{12} appears at 982 cm^{-1}. The number of peaks given by *v* W-O-W in PW_{12} is two, one at 812 cm^{-1} and other at 893cm^{-1}. Symmetric and asymmetric stretch of C-O bonded to Zn is observed at 1583 cm^{-1} and 1374 cm^{-1}. Zn-O streching peak appears around 500 cm^{-1}. In plane C-H bending of benzene ring of ligand is found in region of 1225 to 950 cm^{-1}.[67]

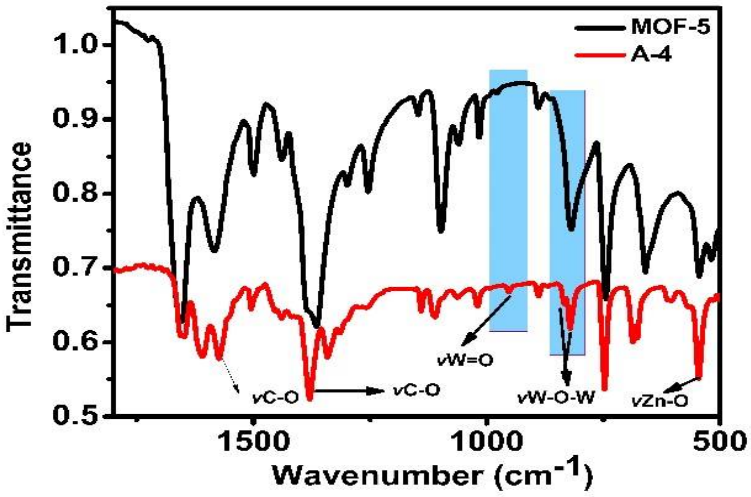

Figure 3.5: FTIR of A-3

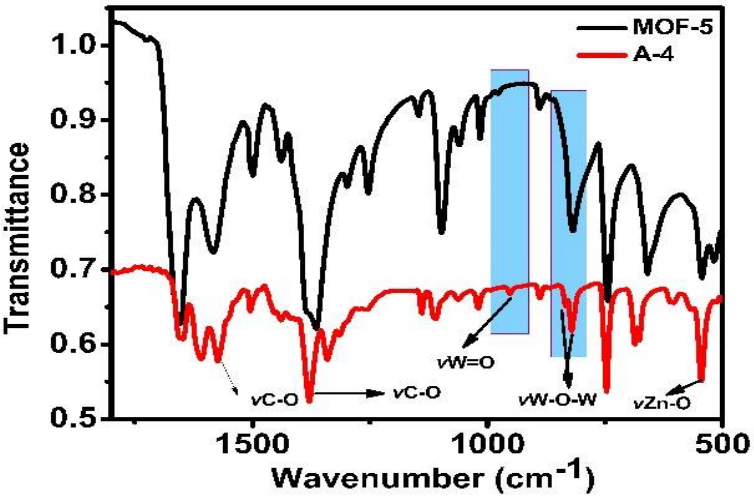

Figure 3.6: FTIR of MOF-5 and A-4

3.3 Elemental Analysis of the Synthesized POMOF Composites:

Elemental analysis of the synthesized POMOF composites by CHN analysis and ICP-MS is shown in table 5 which shows the percentage of elements present in each composite giving idea about confirmation of encapsulation.

Table 5: Elemental analysis of the POMOF composites

Elements	A-1	A-2	A-3	A-4
C	50.51%	27.58%	21.85%	28.32%
H	5.31%	2.95%	1.14%	1.43%
N	29.45%	16.08%	3.64%	0.44%
O	3.2%	12.14%	26.17%	26.13%
Si/P	0.16%	0.6%	0.3%	0.26%
M(Nd /Zn)	0.33%	1.27%	25%	24.68%
W	11.04%	39.36%	21.9%	18.74%

3.4 Thermogravimetric Analysis(TGA) of the Synthesized Composites:

TGA analysis is performed for all the POMOF composites synthesized which are given below;

3.4.1 TGA of A-1:

Figure 3.7 shows the thermogram of ZIF-8 and A-1. Thermogram of ZIF-8 exactly matches with reported ZIF-8 thermogram.[59] Higher weight loss is observed in case of

ZIF-8 as compared to A-1 which indicates that A-1 has loading of POM in it along with ZIF-8.The difference in the thermogram of ZIF-8 and A-1 is 11%. This difference is indicating the loading of PW_{12} in ZIF-8.

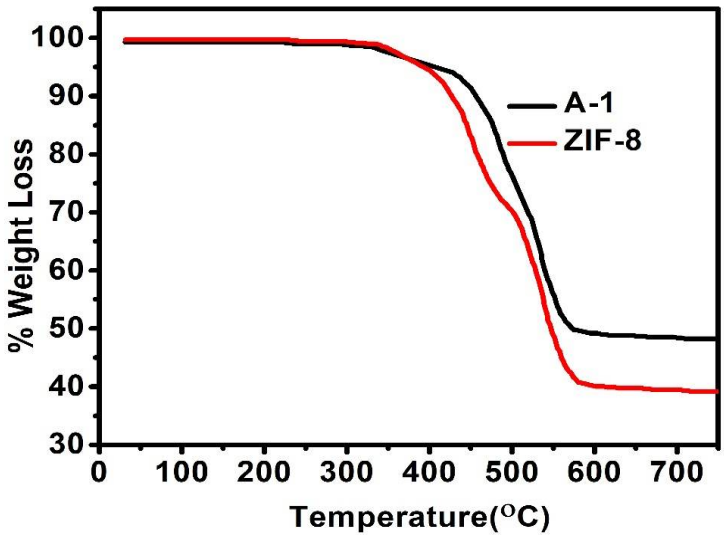

Figure 3.7: TG curve of A-1 and ZIF-8

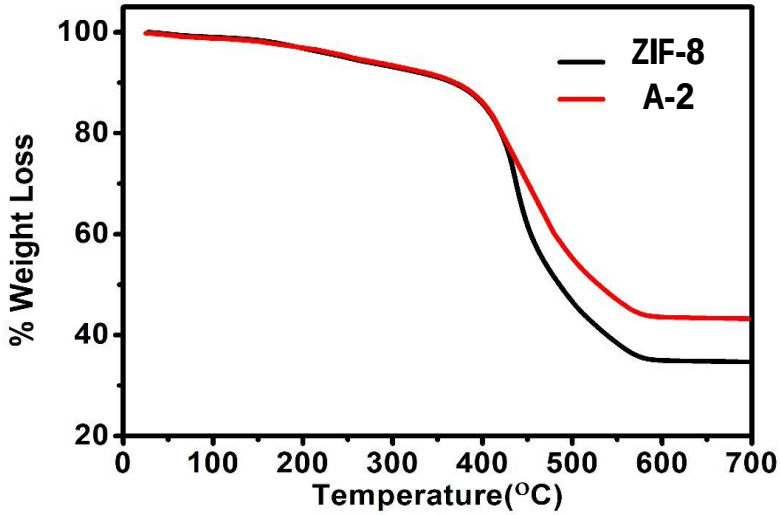

Figure 3.8: TG curve of A-2 and ZIF-8

3.4.2 TGA of A-2:

Figure 3.8 shows the recorded thermogram of ZIF-8 and its composite A-2.The recorded thermogram of ZIF-8 is in agreement with reported one.[59] The difference in percentage weight loss is confirming the loading of PW_{11} in ZIF-8. The loaded percentage on basis of TGA is 9%.

3.4.3 TGA of A-3:

Figure 3.9 shows the TG curve of the Nd MOF alone with its composite A-3. The weight loss took place up to 700 °C is because of the loss of ligand which is organic part of the Nd MOF.[60] The difference in the TG curve of Nd MOF and A-3 indicates the 29% POM loading in the pore cavities of MOF.

3.4.4 TGA of A-4:

Figure 3.10 shows the thermogram of MOF-5 along with its composite A-4. The thermogram of MOF-5 shows agreement with thermogravimetry (TG) curve reported in literature.TG curve shows very small loss of weight up to 200 °C because solvent molecules are removed from cavities of MOF-5, also due to loss of presence of some organic linker moieties on the surface of crystals of MOF-5. The weight loss up to temperature 700 °C is due to the loss of the organic linker i.e. Hmim and ZnO is left.[64]

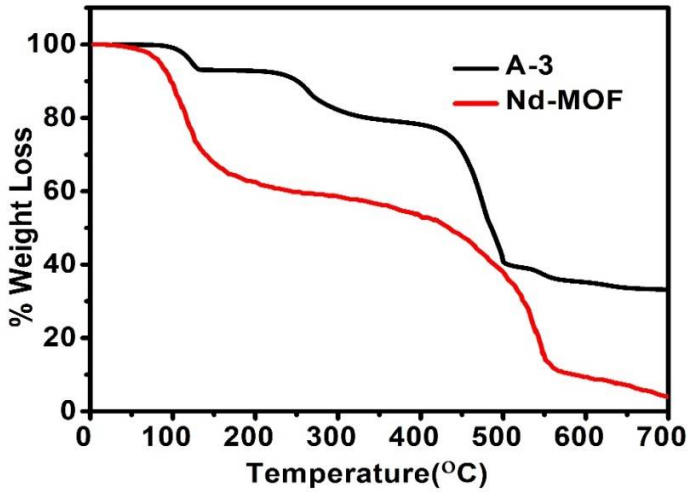

Figure 3.9: TG curve of A-3 and Nd MOF

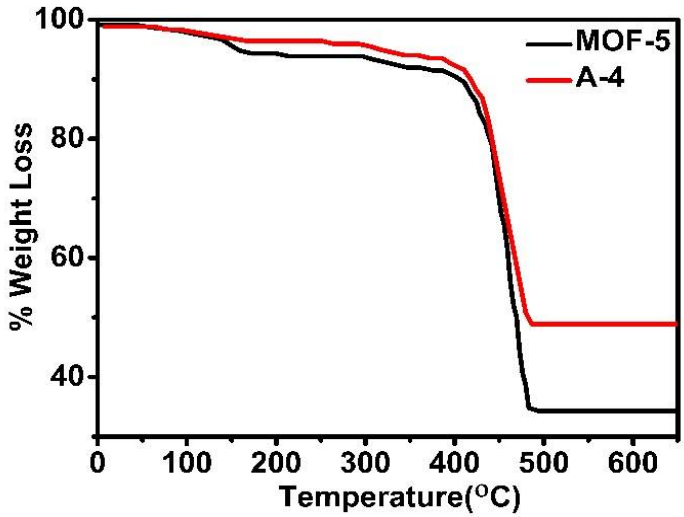

Figure 3.10: TG Curve of A-4 and MOF-5

The difference in the weight loss of MOF-5 and A-4 indicates the encapsulation of POM in the MOF-5. Less weight loss is observed in case of A-4 demonstrating the presence of POM residue along with MOF-5 residue. 25% POM loading is observed in A-4.

3.5 N_2 Adsorption Studies:

Nitrogen adsorption studies give information about;[68]

- pore volume,
- type and number of the pores present in the structure
- decrease in pore volume
- give evidence of encapsulation
- tells about MOF surface area before and after encapsulation

3.5.1 N_2 Adsorption Studies of A-1 and A-2:

Figure 3.11 shows the N_2 adsorption isotherms of ZIF-8 and its composites A-1 and A-2. N_2 adsorption isotherm of ZIF-8 is accordance with reported isotherm of ZIF-8.[59] The decrease in surface area is observed in case of A-1 and A-2 which indicates the encapsulation of PW_{12} and PW_{11} in cavities of ZIF-8, respectively.

3.5.2 N_2 Adsorption Studies of A-4:

Figure 3.12 shows nitrogen adsorption isotherm of MOF-5 and its composite A-4. It tells about the surface area of both MOF-5 and its composite A-4. The isotherm of MOF-5 in the agreement with reported isotherm.[64] The less volume adsorbed of N_2 at 77 K in case of A-4 as compared to MOF-5 which confirms the encapsulation of PW_{12} in the cavities of MOF-5.

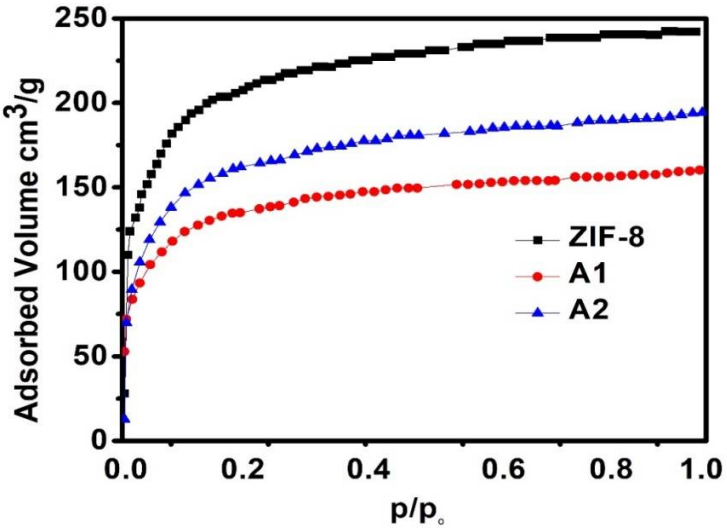

Figure 3.11: N_2 Adsorption Isotherm of A-1 and A-2

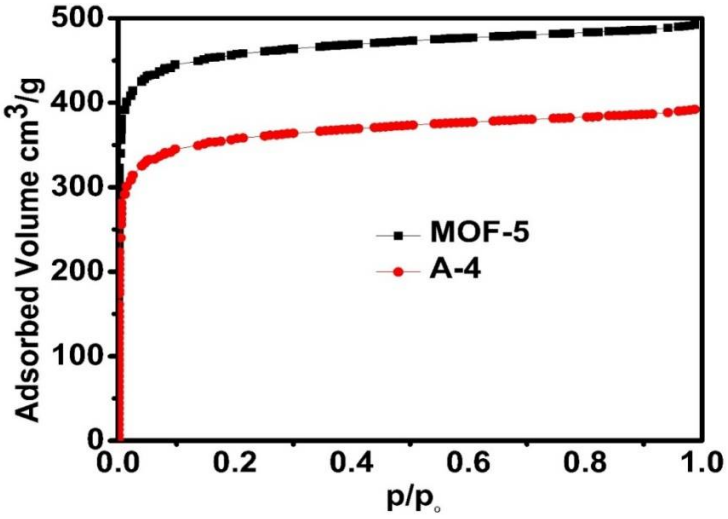

Figure 3.12: N_2 Adsorption isotherm of A-4 and MOF-5

3.6 Suggested Formulae of the Synthesized Composites on basis of TGA:

Based on elemental analysis the suggested formulae of POMOF composites are given in table 6. These calculations are based on comparison of elemental analysis of parent MOFs and POMs alone.

Table 6: Suggested formulae of the POMOF composites on basis of TGA

Sr. No.	Compounds	Formulae	POMs (%age)
1	ZIF-8	$C_8H_{10}N_4Zn$	
2	A-1	$[PW_{12}O_{40}]_{0.14}$@ZIF-8	14%
3	A-2	$[PW_{11}O_{39}]_{0.11}$@ZIF-8	11%
4	Nd MOF	$Nd_8(L)_{12}(H_2O)_8$	
5	A-3	$[SiW_{11}O_{39}]_{0.31}$@Nd MOF	31%
6	MOF-5	$Zn_4O(BDC)_3$	
7	A-4	$[PW_{12}O_{40}]_{0.27}$@MOF-5	27%

3.7 Applications of POMOF Composites:

3.7.1 Catalytic Reduction of 4-Nitrophenol:

Paranitrophenol (4-NP) is prominent industrial pollutant therefore its removal from wastes is necessary and its conversion into the environment friendly products such as Paraaminophenol (4-NP). $NaBH_4$ is used as reducing agent but it does not cause the reduction of 4-NP. Efficient catalyst is required to aid the reduction process. Synthesized

POM-based MOF composites were checked for 4-NP reduction using UV-Visible Spectroscopy as the decrease in 4-nitrophenolate ion peak at 400nm and increase in peak of 4-aminophenol at 290 nm is indicated by UV-Visible spectrophotometer. A-2 was active for almost complete reduction of the 4-NP at pH 5. The general scheme of the reaction is given below:

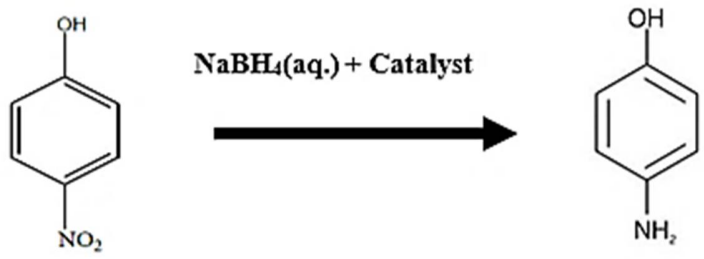

Light yellow 4-nitrophenol aqueous solution shows maximum absorbance peak at 317 nm. On $NaBH_4$ addition colour changes to intense yellow resulting formation of 4-nitrophenolate ion as the absorption peak appears at 400 nm as shown in figure 3.13.[69]

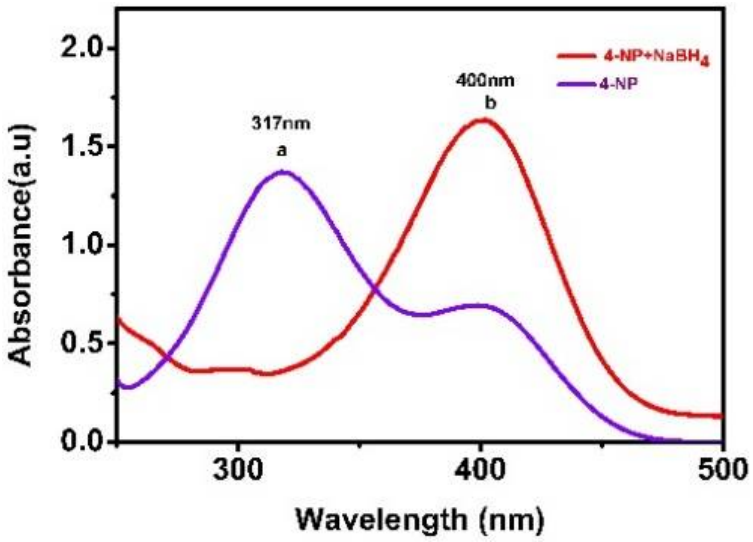

Figure 3.13: UV-Visible spectrum for (a).4-NP (b).Phenolate ion formed on addition of $NaBH_4$

As the sodium borohydride is added in excess, hence rate of reaction is independent of its concentration and depends only on the concentration of 4-NP. So, reduction of 4-NP follows the pseudo-first order kinetics.[70]

$$dcNP/dt = -k_{app.}\, cNP.\, cBH_4^- = -k_{app.}\, cNP$$

Where,

cNP= Concentration of 4-NP

cBH_4 = Concentration of borohydride ion

k_{app}=Apparent rate constant

Rate constant for pseudo-first order reaction has been calculated by plotting UV-Visible data. The graph is plotted between time and ln C_t/ C_o .

And, ln C_t/ C_o = - kt

C_t = Concentration at any time of reaction

C_0= Initial concentration

k=apparent rate constant

t = time required for completion of reaction

3.7.2 Reduction of 4-Nitrophenol in presence of $NaBH_4$ without addition of catalyst:

No reduction of 4-NP was observed on addition of $NaBH_4$ till one hour after addition. It reduces 4-NP too slowly. There was no formation of 4-AP observed in the recorded UV-visible spectrum shown in figure 3.14.

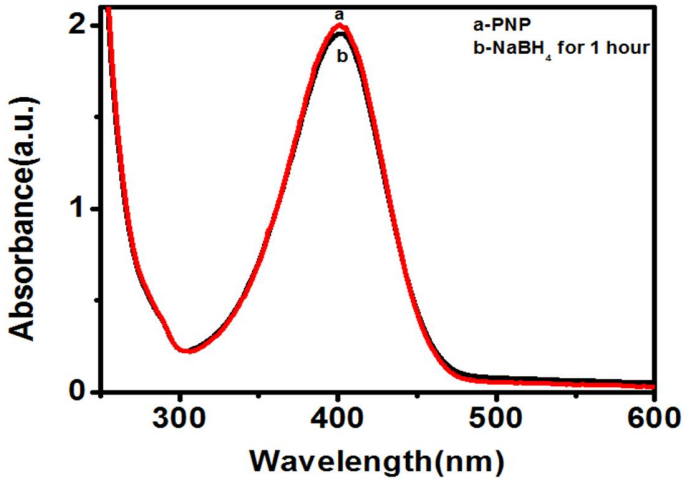

Figure 3.14: Reduction of 4-NP by $NaBH_4$

3.7.3 Catalytic Reduction of 4-NP by A-2:

A-2 shows higher activity as compared to ZIF-8 and PW_{11} alone as shown in figures 3.16 and 3.17, respectively. When 5 mg of the catalyst A-2 are added adjusting the pH at 5 by HCl, 4-NP is reduced to 4-aminophenol as shown in figure 3.18. The schematic diagram of conversion of 4-NP to 4-AP is shown in figure 3.15.

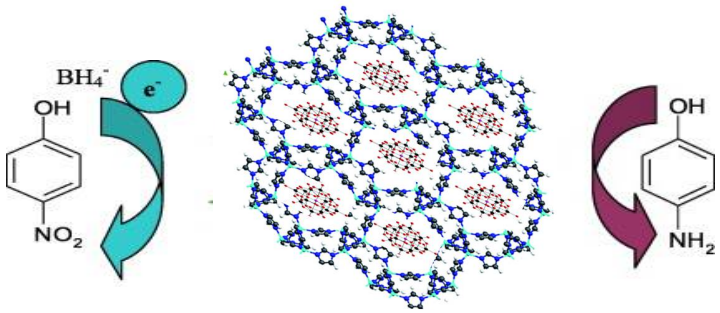

PW_{11}@ZIF-8

Figure 3.15: Schematic diagram of the reaction of 4-NP reduction to 4-AP

Graph is plotted between $\ln C_t/C_o$ V time (min) gives the value of Linear regression (R^2). The straight line equation (y= mx + c) is followed by 4-NP reduction where 'm' is the slope by which rate constant is determined shown in figure 3.19. The product formed after degradation is also confirmed by GC-MS spectrum in figure 3.20. The mechanism

of the reaction can be explained as the both reactants are adsorbing on the catalytic sites of the catalyst and the kinetic barrier is decreased by catalyst hence, electrons are transferred from BH_4^- (which is donor) to 4-NP and 4-NP is reduced to 4-aminophenol(4-NP).[71] By using formula TOF= (number of molecules reacted) / (number of sites)*(time), turn over frequency of the A-2 composite was found to be 225 $Lg^{1-}s^{1-}$.

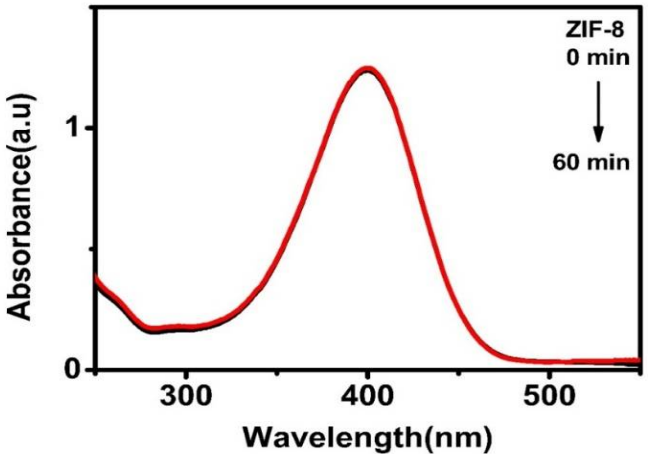

Figure 3.16: 4-NP reduction by ZIF-8

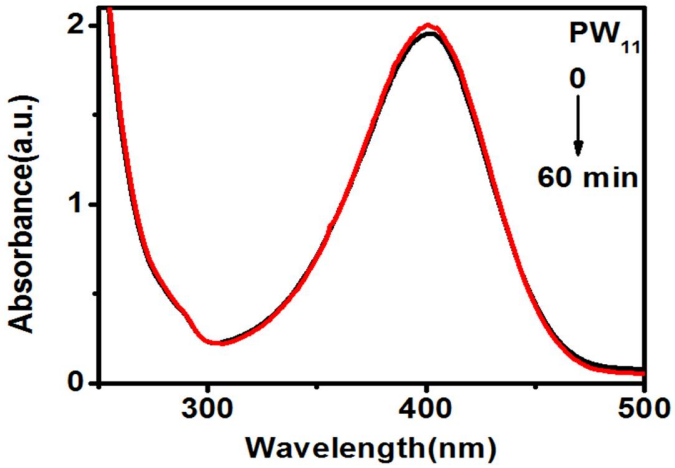

Figure 3.17: 4-NP Reduction by PW_{11}

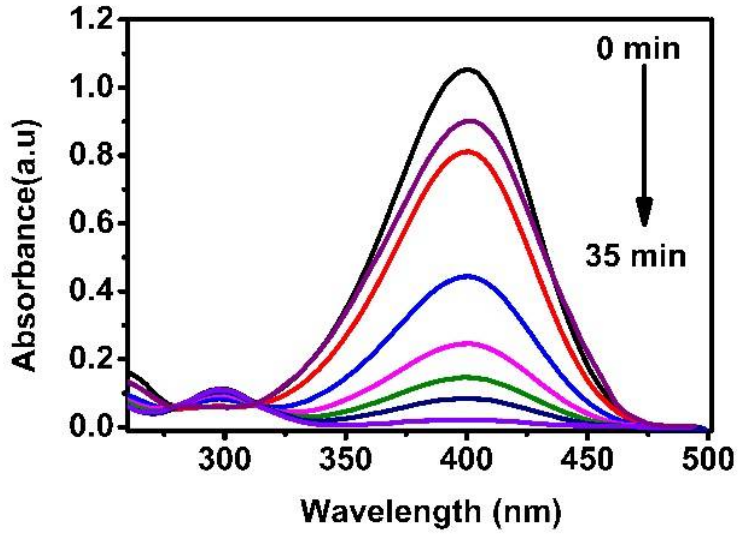

Figure 3.18: 4-NP reduction by A-2 at pH 5

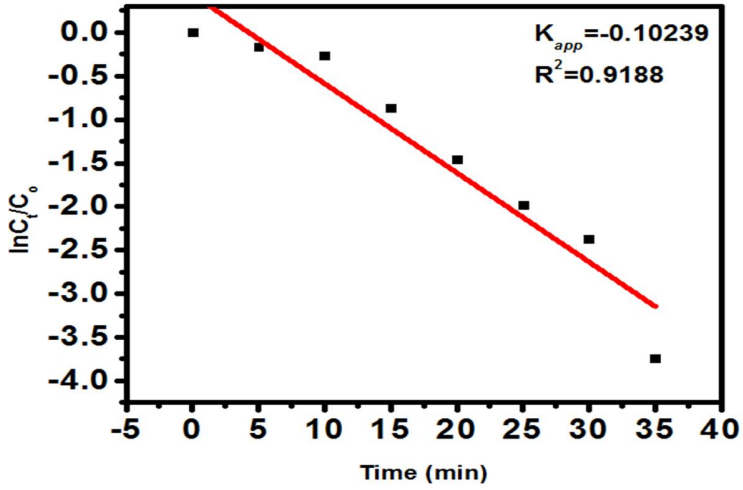

Figure 3.19: Plot of ln C_t/ C_o vs. time showing kinetics of 4-NP in presence of A-2 catalyst

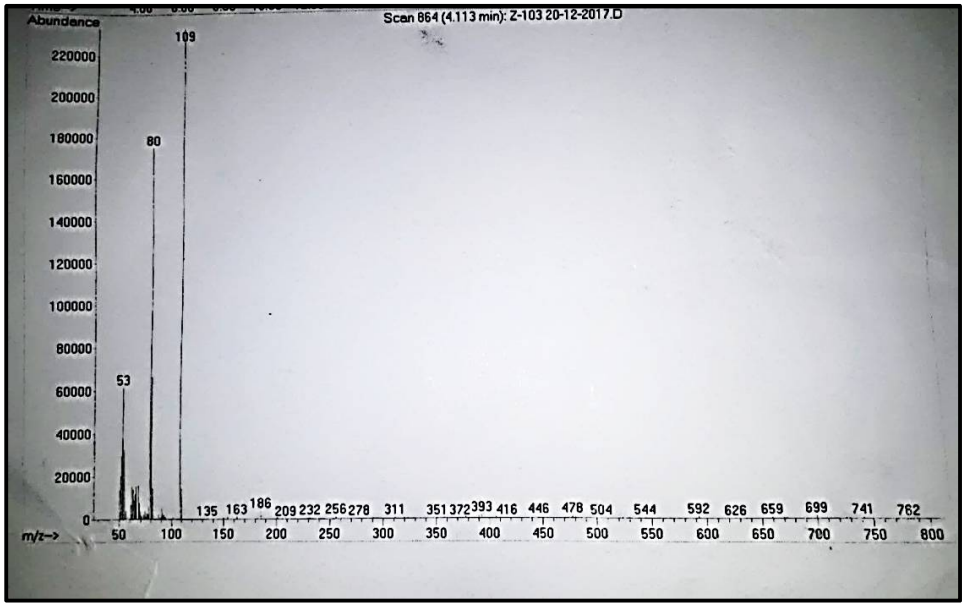

Figure 3.20: GC-MS of the product after the reduction of 4-NP

3.7.4 4-NP reduction by A-3:

A-3 is slightly active for 4-NP reduction. There was no effect of changing pH on catalytic activity of A-3. The activity was observed up to 35 minutes. After 35 minutes no change observed for 2 hours. The recorded spectrum is shown in figure 3.23.

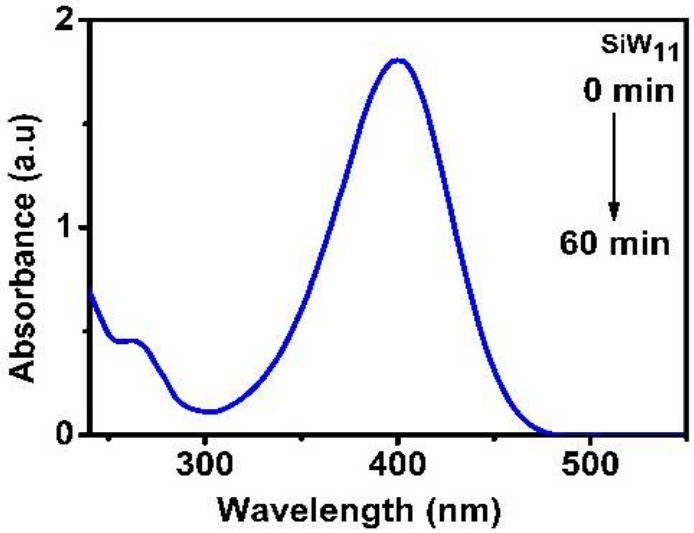

Figure 3.21: 4-NP reduction by SiW_{11} alone

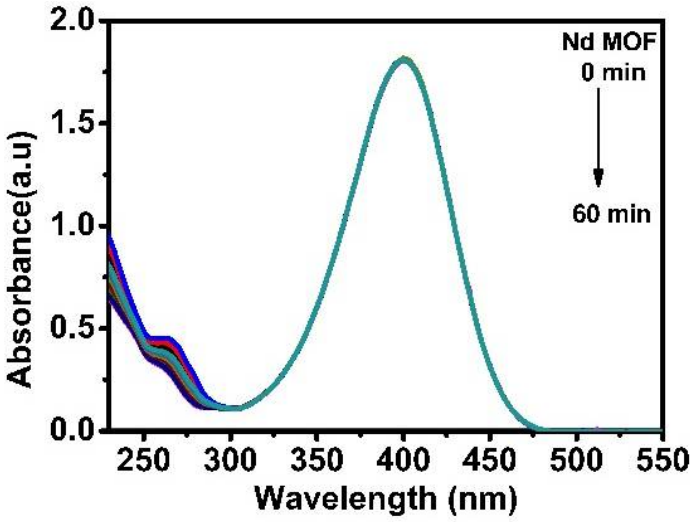

Figure 3.22: 4-NP reduction by Nd MOF

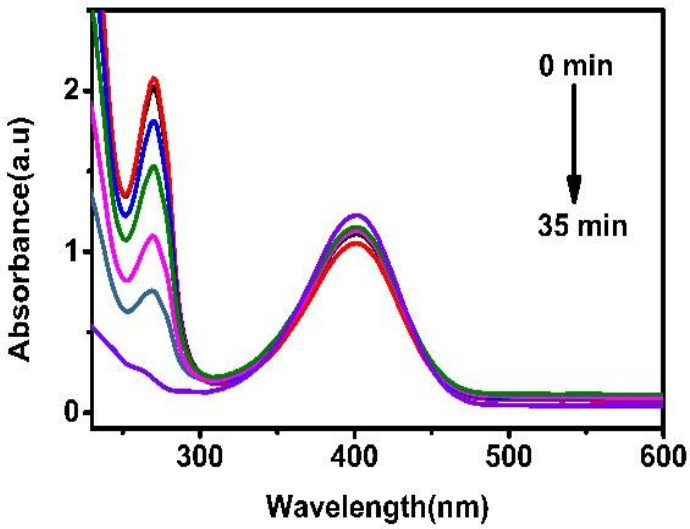

Figure 3.23: 4-NP reduction by A-3

.While Nd MOF and SiW_{11} are inactive as shown in figure 3.22 and 3.21, respectively.

3.7.5 Degradation of Congo Red by the POMOF Composites:

Congo red shows λ_{max} at 497 nm due to presence diazo group. While peaks at 235 nm and 344 nm are due to benzene and naphthalene rings as shown in figure 3.24. It follows

pseudo first order kinetics. Percentage degradation efficiency is determined by using formula:

$$\text{Degradation (\%)} = \frac{C_o - C_t}{C_o} \times 100$$

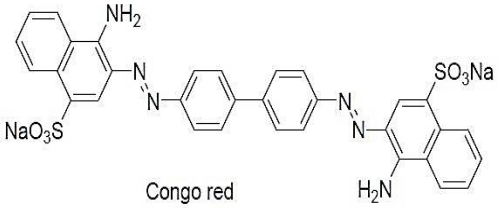

Congo red

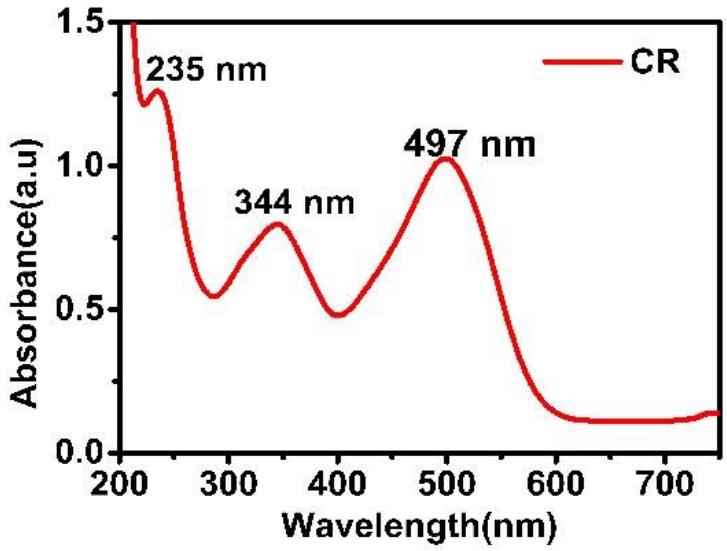

Figure 3.24: UV-Visible spectrum of Congo red

3.7.6 Degradation of Congo red by A-2:

A-2 is active for the degradation of Congo red, it degrades the dye up to 80% in 22 minutes shown in figure 3.25. Percentage degradation is shown in figure 3.26. After 22 minutes there was no degradation observed. It can degrade the dye without the aid of light. Catalyst is catalysing the reaction heterogeneously.

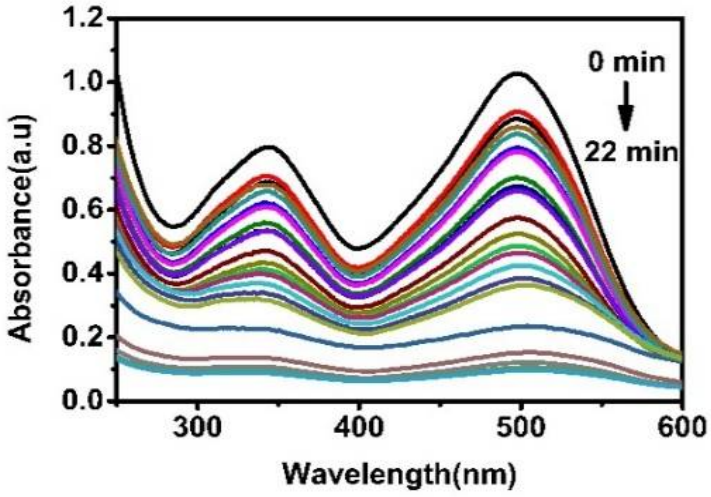

Figure 3.25: UV-Visible spectrum of Congo red degraded by A-2

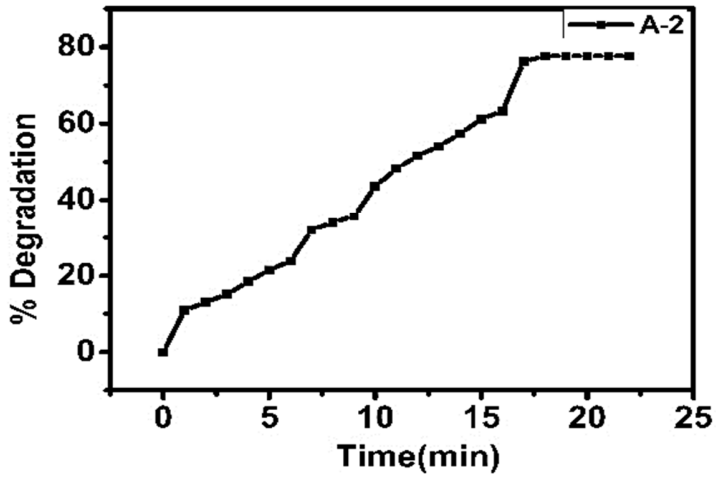

Figure 3.26: Graph of percentage degradation of Congo red by A-2 with time

3.7.7 Degradation of Congo red by A-3:

A-3 is shows catalytic activity for the degradation of Congo red in figure 3.27 and it can degrade it without the aid of light. The percentage dye degradation was 96.6% as shown in figure 3.28. The catalysis carried out by A-3 is heterogeneous catalysis.

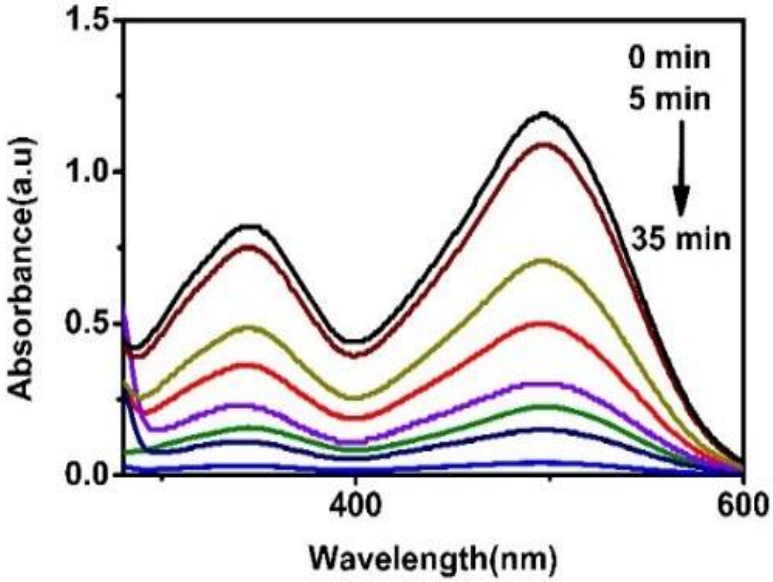

Figure 3.27: UV-Visible spectrum of degradation of Congo red by A-3

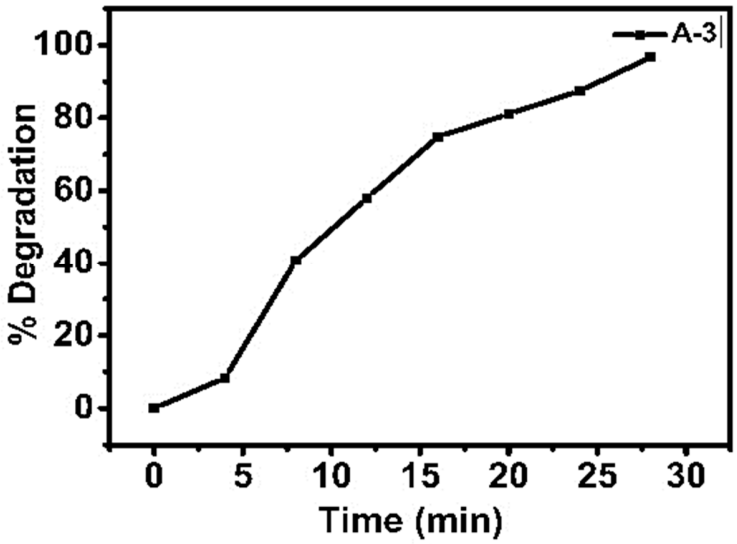

Figure 3.28: Graph of percentage degradation of Congo red by A-3

3.8 Conclusion:

- Four POMOF composites were prepared successfully with significant POMs loading in MOFs.

    1. PW_{12}@ZIF-8 (A-1)
    2. PW_{11}@ZIF-8 (A-2)
    3. SiW_{11}@Nd MOF (A-3)
    4. PW12@MOF-5 (A-4)

- The synthesized composites were characterized by PXRD, FTIR, Elemental Analysis, TGA and N_2 adsorption studies.
- PNP reduction and Congo red dye degradation studies were investigated.
- A-2 and A-3 were found to be active for *p*-nitrophenol reduction, A-2 showed maximum 4-NP degradation at pH 5.
- A-2 and A-3 also showed Congo red degradation.
- They can catalyze the reaction without the aid of light.
- They were found to be more stable and recoverable heterogenous catalyst as compare to bare POMs.
- After encapsulation Homogeneous POMs become heterogeneous catalysts
- Some novel catalytic activity arises in composite material which is absent in its individual components

  In case of 4-NP reduction and Congo red degradation the catalysts are insoluble hence their separation is facile and they can be recovered for reuseability.
- Catalytic activity of POMs is upgraded in many cases after encapsulation.

4 References:

1. Hutin, M.; Rosnes, M.; Long, D.; Cronin, L., 2.10 Polyoxometalates: Synthesis and Structure–From Building Blocks to Emergent Materials. **2013**.
2. Blazevic, A.; Rompel, A., The Anderson–Evans polyoxometalate: From inorganic building blocks via hybrid organic–inorganic structures to tomorrows "Bio-POM". *Coordination Chemistry Reviews* **2016,** *307*, 42-64.
3. Pauling, L., XXIV. The Crystal Structure of the A-Modification of the Rare Earth Sesquioxides. *Zeitschrift für Kristallographie-Crystalline Materials* **1929,** *69* (1-6), 415-421.
4. Tilley, T. D., Molecular design and synthesis of heterogeneous and single-site, supported catalysts. *Journal of Molecular Catalysis A: Chemical* **2002,** *182*, 17-24.
5. Rosnes, M. H.; Yvon, C.; Long, D.-L.; Cronin, L., Mapping the synthesis of low nuclearity polyoxometalates from octamolybdates to Mn-Anderson clusters. *Dalton Transactions* **2012,** *41* (33), 10071-10079.
6. Basset, J.-M.; Candy, J.-P.; Coperet, C.; Lefebvre, F.; Quadrelli, E., Design, Building, Characterization and Performance at the Nanometric Scale of Heterogeneous Catalysts. *Nanotechnology in Catalysis* **2004**, 447-466.
7. Patel, K. R. Managenese substituted polyoxometalates and their functionalization: synthesis, characterization and oxidation of Alkenes. 2014.
8. Kozhevnikov, I. V., Catalysis by heteropoly acids and multicomponent polyoxometalates in liquid-phase reactions. *Chemical Reviews* **1998,** *98* (1), 171-198.
9. Zhang, X.; Anderson, T. M.; Chen, Q.; Hill, C. L., A Baker− Figgis Isomer of Conventional Sandwich Polyoxometalates. H2Na14 [FeIII2 (NaOH2) 2 (P2W15O56) 2], a Diiron Catalyst for Catalytic H2O2-Based Epoxidation. *Inorganic chemistry* **2001,** *40* (3), 418-419.
10. Bardin, B. B.; Bordawekar, S. V.; Neurock, M.; Davis, R. J., Acidity of Keggin-type heteropolycompounds evaluated by catalytic probe reactions, sorption microcalorimetry, and density functional quantum chemical calculations. *The Journal of Physical Chemistry B* **1998,** *102* (52), 10817-10825.
11. Li, G.; Ding, Y.; Wang, J.; Wang, X.; Suo, J., New progress of Keggin and Wells–Dawson type polyoxometalates catalyze acid and oxidative reactions. *Journal of Molecular Catalysis A: Chemical* **2007,** *262* (1-2), 67-76.

12. Tian, A.-x.; Ying, J.; Peng, J.; Sha, J.-q.; Han, Z.-g.; Ma, J.-f.; Su, Z.-m.; Hu, N.-h.; Jia, H.-q., Assembly of the highest connectivity Wells-Dawson polyoxometalate coordination polymer: the use of organic ligand flexibility. *Inorganic chemistry* **2008,** *47* (8), 3274-3283.

13. Cao, R.; Liu, S.; Xie, L.; Pan, Y.; Cao, J.; Ren, Y.; Xu, L., Organic− Inorganic Hybrids Constructed of Anderson-Type Polyoxoanions and Oxalato-Bridged Dinuclear Copper Complexes. *Inorganic chemistry* **2007,** *46* (9), 3541-3547.

14. Kushch, L.; Golhen, S.; Cador, O.; Yagubskii, E.; Il'in, M.; Schaniel, D.; Woike, T.; Ouahab, L., Photochromic Molecular Material Based on Anderson–Evans Polyoxometalate and Ruthenium Mononitrosyl Complexes. *Journal of Cluster Science* **2006,** *17* (2), 303-315.

15. Gómez-García, C. J.; Ouahab, L.; Gimenez-Saiz, C.; Triki, S.; Coronado, E.; Delhaès, P., Coexistence of Mobile and Localized Electrons in Bis (ethylene) dithiotetrathiafulvalene (BEDT-TTF) Radical Salts with Paramagnetic Polyoxometalates: Synthesis and Physical Properties of (BEDT-TTF) 8 [CoW12O40]· 5.5 H2O. *Angewandte Chemie International Edition* **1994,** *33* (2), 223-226.

16. Rohmer, M.-M.; Bénard, M.; Blaudeau, J.-P.; Maestre, J.-M.; Poblet, J.-M., From Lindqvist and Keggin ions to electronically inverse hosts: Ab initio modelling of the structure and reactivity of polyoxometalates. *Coordination chemistry reviews* **1998,** *178*, 1019-1049.

17. Sun, C.-Y.; Liu, S.-X.; Liang, D.-D.; Shao, K.-Z.; Ren, Y.-H.; Su, Z.-M., Highly stable crystalline catalysts based on a microporous metal− organic framework and polyoxometalates. *Journal of the American Chemical Society* **2009,** *131* (5), 1883-1888.

18. Savova, B. Étude du dopage de catalyseurs de déshydrogénation oxydante de l'éthane et du propane. Université Claude Bernard-Lyon I; l'Institut de Recherches sur la Catalyse de Sofia, 2009.

19. Wei, M.; He, C.; Sun, Q.; Meng, Q.; Duan, C., Zeolite ionic crystals assembled through direct incorporation of polyoxometalate clusters within 3D metal-organic frameworks. *Inorganic chemistry* **2007,** *46* (15), 5957-5966.

20. Shimizu, K.-i.; Furukawa, H.; Kobayashi, N.; Itaya, Y.; Satsuma, A., Effects of Brønsted and Lewis acidities on activity and selectivity of heteropolyacid-based catalysts for hydrolysis of cellobiose and cellulose. *Green Chemistry* **2009,** *11* (10), 1627-1632.

21. Shimizu, K.-i.; Niimi, K.; Satsuma, A., Polyvalent-metal salts of heteropolyacid as efficient heterogeneous catalysts for Friedel–Crafts acylation of arenes with carboxylic acids. *Catalysis Communications* **2008,** *9* (6), 980-983.

22. Kamata, K.; Sugahara, K., Base Catalysis by Mono-and Polyoxometalates. *Catalysts* **2017,** *7* (11), 345.

23. Khan, M. I.; Chen, Q.; Zubieta, J., Hydrothermal synthesis and crystal and molecular structure of a reduced, arsenic rich heteropolyanion, Na 4 [Mo 4 As 6 O 20 (OH) 2]· 9H 2 O. *Journal of the Chemical Society, Chemical Communications* **1993,** (4), 356-357.

24. Kozhevnikov, I.; Matveev, K., Homogeneous catalysts based on heteropoly acids (review). *Applied Catalysis* **1983,** *5* (2), 135-150.

25. Chen, J.-J., Polyoxometalate Related Redox Flow Batteries. **2017**.

26. Rhule, J. T.; Hill, C. L.; Judd, D. A.; Schinazi, R. F., Polyoxometalates in medicine. *Chemical Reviews* **1998,** *98* (1), 327-358.

27. Gómez-Romero, P.; Chojak, M.; Cuentas-Gallegos, K.; Asensio, J. A.; Kulesza, P. J.; Casañ-Pastor, N.; Lira-Cantú, M., Hybrid organic–inorganic nanocomposite materials for application in solid state electrochemical supercapacitors. *Electrochemistry Communications* **2003,** *5* (2), 149-153.

28. Hill, C. L., Progress and challenges in polyoxometalate-based catalysis and catalytic materials chemistry. *Journal of Molecular Catalysis A: Chemical* **2007,** *262* (1-2), 2-6.

29. Shimizu, K.-i.; Satsuma, A., Toward a rational control of solid acid catalysis for green synthesis and biomass conversion. *Energy & Environmental Science* **2011,** *4* (9), 3140-3153.

30. Song, J.; Luo, Z.; Britt, D. K.; Furukawa, H.; Yaghi, O. M.; Hardcastle, K. I.; Hill, C. L., A multiunit catalyst with synergistic stability and reactivity: A

polyoxometalate–metal organic framework for aerobic decontamination. *Journal of the American Chemical Society* **2011,** *133* (42), 16839-16846.

31. Chughtai, A. H.; Ahmad, N.; Younus, H. A.; Laypkov, A.; Verpoort, F., Metal–organic frameworks: versatile heterogeneous catalysts for efficient catalytic organic transformations. *Chemical Society Reviews* **2015,** *44* (19), 6804-6849.

32. Chae, H. K.; Eddaoudi, M.; Kim, J.; Hauck, S. I.; Hartwig, J. F.; O'Keeffe, M.; Yaghi, O. M., Tertiary Building Units: Synthesis, Structure, and Porosity of a Metal− Organic Dendrimer Framework (MODF-1). *Journal of the American Chemical Society* **2001,** *123* (46), 11482-11483.

33. Claessens, C. G.; Stoddart, J. F., π-π interactions in self-assembly. *Journal of physical organic chemistry* **1997,** *10* (5), 254-272.

34. Chen, B.; Liang, C.; Yang, J.; Contreras, D. S.; Clancy, Y. L.; Lobkovsky, E. B.; Yaghi, O. M.; Dai, S., A Microporous Metal–Organic Framework for Gas-Chromatographic Separation of Alkanes. *Angewandte Chemie* **2006,** *118* (9), 1418-1421.

35. Furukawa, H.; Cordova, K. E.; O'Keeffe, M.; Yaghi, O. M., The chemistry and applications of metal-organic frameworks. *Science* **2013,** *341* (6149), 1230444.

36. Lee, J.; Farha, O. K.; Roberts, J.; Scheidt, K. A.; Nguyen, S. T.; Hupp, J. T., Metal–organic framework materials as catalysts. *Chemical Society Reviews* **2009,** *38* (5), 1450-1459.

37. Nelson, A. P.; Farha, O. K.; Mulfort, K. L.; Hupp, J. T., Supercritical processing as a route to high internal surface areas and permanent microporosity in metal− organic framework materials. *Journal of the American Chemical Society* **2008,** *131* (2), 458-460.

38. Corma, A.; García, H.; Llabrés i Xamena, F., Engineering metal organic frameworks for heterogeneous catalysis. *Chemical reviews* **2010,** *110* (8), 4606-4655.

39. Chaemchuen, S.; Kabir, N. A.; Zhou, K.; Verpoort, F., Metal–organic frameworks for upgrading biogas via CO 2 adsorption to biogas green energy. *Chemical Society Reviews* **2013,** *42* (24), 9304-9332.

40. Chaemchuen, S.; Zhou, K.; Kabir, N. A.; Chen, Y.; Ke, X.; Van Tendeloo, G.; Verpoort, F., Tuning metal sites of DABCO MOF for gas purification at ambient conditions. *Microporous and Mesoporous Materials* **2015,** *201*, 277-285.

41. Wang, P.; Fan, R.-Q.; Yang, Y.-L.; Liu, X.-R.; Xiao, P.; Li, X.-Y.; Hasi, W.; Cao, W.-W., 1-D helical chain, 2-D layered network and 3-D porous lanthanide–organic frameworks based on multiple coordination sites of benzimidazole-5, 6-dicarboxylic acid: synthesis, crystal structure, photoluminescence and thermal stability. *CrystEngComm* **2013,** *15* (22), 4489-4506.

42. Wang, C.; Xie, Z.; deKrafft, K. E.; Lin, W., Doping metal–organic frameworks for water oxidation, carbon dioxide reduction, and organic photocatalysis. *Journal of the American Chemical Society* **2011,** *133* (34), 13445-13454.

43. Horcajada, P.; Chalati, T.; Serre, C.; Gillet, B.; Sebrie, C.; Baati, T.; Eubank, J. F.; Heurtaux, D.; Clayette, P.; Kreuz, C., Porous metal–organic-framework nanoscale carriers as a potential platform for drug delivery and imaging. *Nature materials* **2010,** *9* (2), 172.

44. Kreno, L. E.; Leong, K.; Farha, O. K.; Allendorf, M.; Van Duyne, R. P.; Hupp, J. T., Metal–organic framework materials as chemical sensors. *Chemical reviews* **2011,** *112* (2), 1105-1125.

45. Kurmoo, M., Magnetic metal–organic frameworks. *Chemical Society Reviews* **2009,** *38* (5), 1353-1379.

46. Horcajada, P.; Gref, R.; Baati, T.; Allan, P. K.; Maurin, G.; Couvreur, P.; Ferey, G.; Morris, R. E.; Serre, C., Metal–organic frameworks in biomedicine. *Chemical reviews* **2011,** *112* (2), 1232-1268.

47. Sachse, A.; Ameloot, R.; Coq, B.; Fajula, F.; Coasne, B.; De Vos, D.; Galarneau, A., In situ synthesis of Cu–BTC (HKUST-1) in macro-/mesoporous silica monoliths for continuous flow catalysis. *Chemical Communications* **2012,** *48* (39), 4749-4751.

48. Pérez-Mayoral, E.; Čejka, J., [Cu3 (BTC) 2]: a metal–organic framework catalyst for the Friedländer reaction. *ChemCatChem* **2011,** *3* (1), 157-159.

49. Song, Y.-F.; Tsunashima, R., Recent advances on polyoxometalate-based molecular and composite materials. *Chemical Society Reviews* **2012,** *41* (22), 7384-7402.

50. Mateo, C.; Palomo, J. M.; Fernandez-Lorente, G.; Guisan, J. M.; Fernandez-Lafuente, R., Improvement of enzyme activity, stability and selectivity via

immobilization techniques. *Enzyme and microbial technology* **2007,** *40* (6), 1451-1463.

51. Soler-Illia, G. J. d. A.; Sanchez, C.; Lebeau, B.; Patarin, J., Chemical strategies to design textured materials: from microporous and mesoporous oxides to nanonetworks and hierarchical structures. *Chemical reviews* **2002,** *102* (11), 4093-4138.

52. Genna, D. T.; Wong-Foy, A. G.; Matzger, A. J.; Sanford, M. S., Heterogenization of homogeneous catalysts in metal–organic frameworks via cation exchange. *Journal of the American Chemical Society* **2013,** *135* (29), 10586-10589.

53. Arico, A. S.; Bruce, P.; Scrosati, B.; Tarascon, J.-M.; Van Schalkwijk, W., Nanostructured materials for advanced energy conversion and storage devices. *Nature materials* **2005,** *4* (5), 366.

54. Imperor-Clerc, M.; Davidson, P.; Davidson, A., Existence of a microporous corona around the mesopores of silica-based SBA-15 materials templated by triblock copolymers. *Journal of the American Chemical Society* **2000,** *122* (48), 11925-11933.

55. Zhou, Y.; Chen, G.; Long, Z.; Wang, J., Recent advances in polyoxometalate-based heterogeneous catalytic materials for liquid-phase organic transformations. *RSC Advances* **2014,** *4* (79), 42092-42113.

56. Stock, N.; Biswas, S., Synthesis of metal-organic frameworks (MOFs): routes to various MOF topologies, morphologies, and composites. *Chemical reviews* **2011,** *112* (2), 933-969.

57. Juan-Alcañiz, J.; Gascon, J.; Kapteijn, F., Metal–organic frameworks as scaffolds for the encapsulation of active species: state of the art and future perspectives. *Journal of Materials Chemistry* **2012,** *22* (20), 10102-10118.

58. He, Z.; Pang, Q.; Rankine, D.; Sumby, C. J.; Zhang, L.; Doonan, C. J.; Li, Q., Encapsulation of polyoxometalates within layered metal–organic frameworks with topological and pore control. *CrystEngComm* **2013,** *15* (45), 9340-9343.

59. Park, K. S.; Ni, Z.; Côté, A. P.; Choi, J. Y.; Huang, R.; Uribe-Romo, F. J.; Chae, H. K.; O'Keeffe, M.; Yaghi, O. M., Exceptional chemical and thermal stability of zeolitic imidazolate frameworks. *Proceedings of the National Academy of Sciences* **2006,** *103* (27), 10186-10191.

60. Zhu, W.-H.; Zeng, M.; Wang, J.; Li, C.-Y.; Tian, L.-H.; Yin, J.-C.; Liu, Y.-K., A multifunctional lanthanide metal–organic framework supported by Keggin type polyoxometalates. *Dalton Transactions* **2016,** *45* (25), 10141-10145.

61. Dinca, M.; Yu, A. F.; Long, J. R., Microporous metal− organic frameworks incorporating 1, 4-benzeneditetrazolate: Syntheses, structures, and hydrogen storage properties. *Journal of the American Chemical Society* **2006,** *128* (27), 8904-8913.

62. Hinterholzinger, F. M.; Ranft, A.; Feckl, J. M.; Rühle, B.; Bein, T.; Lotsch, B. V., One-dimensional metal–organic framework photonic crystals used as platforms for vapor sorption. *Journal of Materials Chemistry* **2012,** *22* (20), 10356-10362.

63. Wang, C.; Zhang, H.; Feng, C.; Gao, S.; Shang, N.; Wang, Z., Multifunctional Pd@ MOF core–shell nanocomposite as highly active catalyst for p-nitrophenol reduction. *Catalysis Communications* **2015,** *72*, 29-32.

64. Cravillon, J.; Münzer, S.; Lohmeier, S.-J.; Feldhoff, A.; Huber, K.; Wiebcke, M., Rapid room-temperature synthesis and characterization of nanocrystals of a prototypical zeolitic imidazolate framework. *Chemistry of Materials* **2009,** *21* (8), 1410-1412.

65. Liu, J.; He, J.; Wang, L.; Li, R.; Chen, P.; Rao, X.; Deng, L.; Rong, L.; Lei, J., NiO-PTA supported on ZIF-8 as a highly effective catalyst for hydrocracking of Jatropha oil. *Scientific reports* **2016,** *6*, 23667.

66. Hu, Y.; Kazemian, H.; Rohani, S.; Huang, Y.; Song, Y., In situ high pressure study of ZIF-8 by FTIR spectroscopy. *Chemical communications* **2011,** *47* (47), 12694-12696.

67. Iswarya, N.; Kumar, M.; Rajan, K.; Balaguru, R., Synthesis, characterization and adsorption capability of MOF-5. *Asian Journal of Scientific Research* **2012,** *5* (4), 247.

68. Lippens, B. C.; De Boer, J., Studies on pore systems in catalysts: V. The t method. *Journal of Catalysis* **1965,** *4* (3), 319-323.

69. Butun, S.; Sahiner, N., A versatile hydrogel template for metal nano particle preparation and their use in catalysis. *Polymer* **2011,** *52* (21), 4834-4840.

70. Esumi, K.; Miyamoto, K.; Yoshimura, T., Comparison of PAMAM–Au and PPI–Au nanocomposites and their catalytic activity for reduction of 4-nitrophenol. *Journal of colloid and interface science* **2002,** *254* (2), 402-405.

71. Dong, Z.; Le, X.; Liu, Y.; Dong, C.; Ma, J., Metal organic framework derived magnetic porous carbon composite supported gold and palladium nanoparticles as highly efficient and recyclable catalysts for reduction of 4-nitrophenol and hydrodechlorination of 4-chlorophenol. *Journal of Materials Chemistry A* **2014,** *2* (44), 18775-18785.